A Cyber-Physical Framework for MRI Guided Magnetic Nano/Micro particles

A Thesis Presented

By

Mani Ahmadniaroudsari

To

The Department of Mechanical and Industrial Engineering

In partial fulfillment of the requirements for the degree of Master of Science

In

Mechanical Engineering

Northeastern University

Boston, Massachusetts

August, 2015

Abstract

Recent research based on phantom and clinical studies, has shown that Magnetic Resonance Imaging (**MRI**) can be employed to navigate and target drug-loaded magnetic micro particles to deep-seated lesions in the human body. This method is based on using the MRI machine as the propulsion force to guide the magnetic micro particles through the intravascular system of the human or animal body.

Here we investigate the feasibility of extending these steering systems to magnetic nanoparticle systems. Simulations indicate that flow and Brownian disruptions dominate the energy landscape in Nano regime. However we have found that we can benefit from the tendency of magnetic nanoparticles to aggregate under applied fields to form larger aggregates to drive our system.

We have conducted both experiment and simulation on how magnetic in-vitro will aggregate in the presence of a fixed magnetic field and can move in fluidic flow and concentrate due to the magnetic field gradients. In this work we compare our simulation against simple validating experiments of flow channels subject to controlled magnetic fields and field gradients. Overall, we find that under certain circumstances we are able to aggregate them into larger clusters to enhance their magnetic response, track velocity of the chainlike aggregates by simulations and validate them with experiments.

Contents

I. Acknowledgments

First, I must thank my previous advisor, Dr. Constantinos Mavroidis. His knowledge and guidance throughout my Master program has been undeniable. I enjoyed his course in the first semester of my master program and that course motivated me to start working in Bio mechatronics lab of his and finally the hard work paid off and we got awarded as a winner for the NSF grant "A Cyber-Physical Framework for MRI Guided Magnetic Nanoparticles".

After the tragedy of Professor Mavroidis Leaving us, I started to work under the supervision of Professor Erb in DAPS group. With his guidelines I could finally satisfy the requirements of Northeastern University to be eligible to Graduate for Master's Program.

I owe Dr. Panagiotis Vertholomeus and Christos Bergeles a great debt of gratitude. They offered their experience and advice to help define the focus and goals of the project.

I cannot begin to express the support I've received from my lab mates in my time in the Biomedical Mechatronics Laboratory. To the senior members, Dr. Rich Ranky, Dr. Maciej Pietrusinski, Dr. Mark Sivak, and Dr. Ozer Unluhisarcikli, and the new members, Patrick Murphy, Yu Pu, Qing Chao 'Andy' Kong, Lexi Carver, Sean Suri, Amir Farjadian, and Elias Brassitos, thank you. I have learned so much from all of you.

Also I have to mention the Lab mates I got to meet and work with in the DAPS group whom where so supportive and nice to me; Joshua Martin, Rasam Soheilian, Jessica Faust, Jabulani Barber and Chunzoul Pan.

Most importantly, I must thank my family. Thank you Mom, Dad and my sister Saina. I would never have gotten this far without your unconditional support.

II. Introduction

Approximately 7.6 million people die from cancer each year according to an article titled "ACS Report Focuses on Global Cancer Toll". Surgery, Radiation treatment, Chemotherapy, Immunotherapy, Hormonal therapy and Stem cell/bone marrow transplantation are typically being performed to treat cancer patients. All these methods has been proven to be high risk and has a lot of side effects mostly causing patients to die after couple of months of the operation. My former adviser Professor Mavroidis himself was a victim of one of this methods of treatment. So finding out new methods to avoid the side effects of the current ones seems to have the highest impact on day to day life of human beings.

In 2004 MRI Guided drug delivery was proposed as a new method for cancer treatment by *Sylvian Martel* and *Constantinos Mavroidis*. The method was based on using the MRI machine as the propulsion force to guide the magnetic Nano/Micro particles through the intravascular system of the human or animal body. MRI machines have the advantage to simultaneously perform imaging and targeting while covering the whole frame of the body of a person. Furthermore, MRI machines have different coil types that can be used to generate both fixed fields and field gradients simultaneously, which enable the guidance of magnetic particles along the intravascular system. By injecting Nano/Micro Particles to the body and get them aggregated by fixed field of MRI, then target them aggregations along 3D directions using magnetic gradients of the MRI the Particles would aggregate because of their dipolar interactions and would repel each other at close distance due to their steric properties. Particles aggregation can be beneficial because less magnetic field and gradients would be needed for targeting and steering comparing to a single particle. On the other hand aggregates can`t be dispersedly guided and get to the cancer region when the cancer tumor is located in thin capillaries.

Researchers have performed experiments using MRI machine and simulations validating the results in Micro scale. But as a researcher I believe this topics is open-ended for all to follow and continue especially going to smaller scale as Nano for the following reasons:

- Tissue permeation
- Cell phagocytosis
- Clotting Avoidance

Development of a simulation tool for examining the physical parameters that affect the aggregation/breakup process potentially is the main target in this topic while existing SW packages

were based either on Finite Element Methods or on Molecular dynamics, and none of these provide functionalities allowing to study efficiently the dynamic behavior of interacting magnetic rigid bodies subject to forces arising from different physical domains at the Nano scale. So determining how the Nano particle properties could be controlled, Processed and targeted easily in major vessel bifurcations by performing post processing, Simulation and visualization of the magnetic Nano Particles in fluidic environments is the future in this area of research.

Professor Mavroidis Research team were employing a cluster parallel type of programming system using Visual Studio and MATLAB software to simulate and visualize the Micro/Nano Particles Aggregation movement and potentially combine this as a singular software that can be used in laboratories or Research facilities as the property of Northeastern university which can visually show the movement of particles aggregation and guide them to the target which would be the cancer tumor while giving feed back to the user of the Forces plots and desired trajectories.

Starting my new era of research In DAPS group I realized the steps that has to perform for this idea with a different method and approach by trying to model the Dynamics of particle aggregation starting two particles in MATLAB and visualize them in OVITO.

In both cases the plan should be to gather big data libraries of the steering guideline and trajectories with control algorithm involved for variety of particles sizes and gather them all in a data base so the user just reaches for his desired properties in this vast library of information.

This plan would need a group of researchers to import the finalize MATLAB codes to a cluster type of computing system which would run daily with less time consumption and stores the data in the source data library for future need.

So as a part of this I have been finding a model that can be properly used to simulate the aggregation of particles in advance and then manage to look for big data in this subject.

At the time while there was no easy access to the MRI machine we started to develop our experimental setup validating our simulation simply by remodeling the MRI machine in a very smaller scale using solenoids, Microscope and microfluidic channels to study the aggregation process in reality. [1,2,3,4,5,6,7,8,9,10,11,12,13]

III.   Contributions

The main contributions of this thesis are:

- The novel idea of the Simulation Platform that can be used to process and visualize the movement of Micro/Nano particles in a fluidic environment.

- The ability to access to all forces and torques implemented on each particle in each time step during the simulation time.

- The ability to control and design guidelines for the particles to follow the assigned trajectories.

As a results of this work, the following publications are in preparation:

- M.Ahmadniaroudsari and C. Mavroidis, "In-Silico studies of magnetic nanoparticles aggregation in a fluidic environment" *IEEE Transactions on Nanoparticles*, 2014.

- Enhanced 'Stearability' of Magnetic particles (in-vivo) via aggregation. Summer 2015

IV.   Background

Any overview on drug delivery should start with the deserved recognition of Paul Ehrlich (1854-1915), who proposed that if an agent could selectively target a disease-causing organism, then a toxin for that organism could be delivered along with the agent of selectivity. Ehrlich received the 1908 Nobel Prize in Medicine for his work in the field of immunity. Since then, various strategies have been proposed to deliver a drug to the vicinity of a tumor.

Magnetic field can be recognized as the physical stimuli which can be used to manipulate the movement of the object that has the magnetic properties. Magnetic Micro/Nano particles are the targets for this method of drug delivery.

Magnetic micro particles initially were proposed as contrast agents for localized radiation therapy and to induce vascular occlusion of the tumors.

Drug delivery has been improved through time by several of different methods. In my thesis Nano robotic drug delivery system guided by magnetic resonance imaging (MRI) scanner has been proposed for targeted drug delivery in the human body. The expectation is that it will achieve substantially increased rates of therapeutic and diagnostic success compared with conventional methods.

The drug delivery systems based on the use of Nano/Micro particles has significant advantages such as:

(i)   The ability to target specific locations in the body;

(ii)   The reduction of the quantity of drug needed to attain a particular concentration in the vicinity of the target;

(iii)   The reduction of the concentration of the drug at non target sites minimizing severe side effects. All these benefits justify the exponential growth in the number of publications dealing with NPs for drug delivery applications.

The main limitation of magnetic drug delivery relates to the strength of the external field that can be applied to obtain the necessary magnetic gradient to control the residence time of nanoparticles in the desired area or which triggers the drug desorption. [1,2,3,4,5,6,7,8,9,10,11,12,13]

1) OVERVIEW OF THE MRI DRUG DELIVERY SYSTEM ARCHITECTURE

The architecture of the MRI-based Nano robotic system is shown in Figure 1. The most critical components of the architecture of MRI-guided nanorobotic system are described at the following.
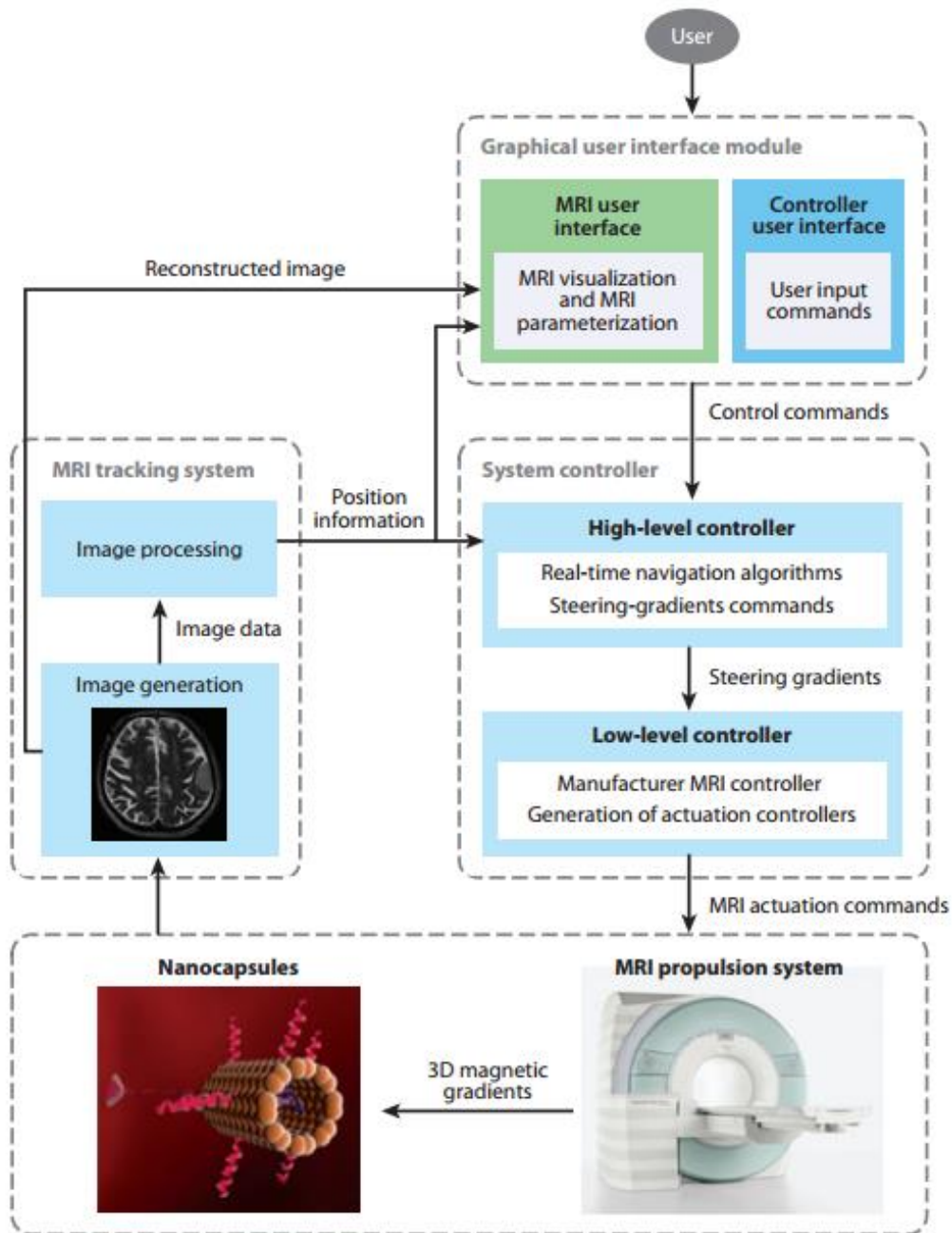
*Figure 1- MRI-guided Nanorobotic system architecture (**Reference 2**). Shows that the desired MRI system consists of MRI Propulsion system, MRI tracking system, System controller and Graphical User interface that together work as a feedback control system that could design trajectories guidelines and target the particles to the desired region of Human Body.*

(a)   Nano capsule

The nano capsule is the most important sub system of the MRI-based nanorobotic architecture. Its components are described below. [2, 3, 4, 5, 19]
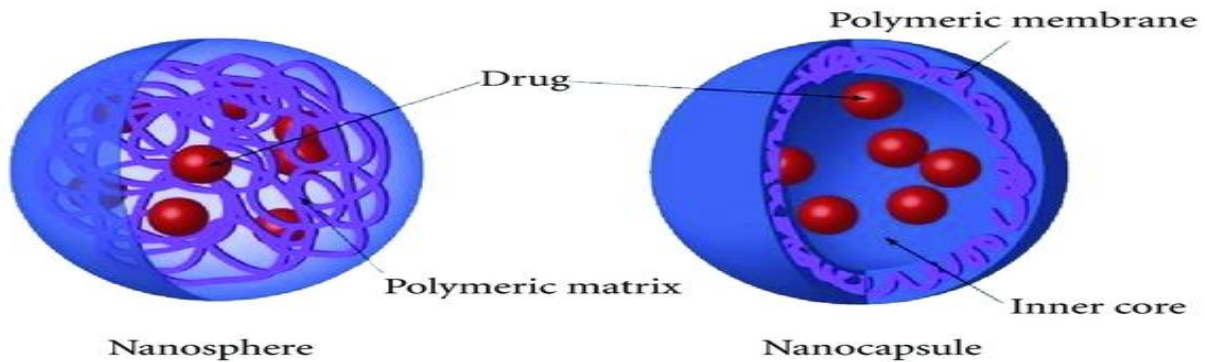
*Figure 2-The structure of the Nano capsule used for drug delivery- (**Reference 38**). Consist of a Polymeric Membrane and the inner core which would filled with the drug. The membrane could be made of IRON Oxide or Cobalt as well.*

(b)   MRI Propulsion System

Every MRI installation will contain at least the following main hardware building blocks. Their functionality is shared by the propulsion system and the tracking system. [2, 3, 4, 5, 19]
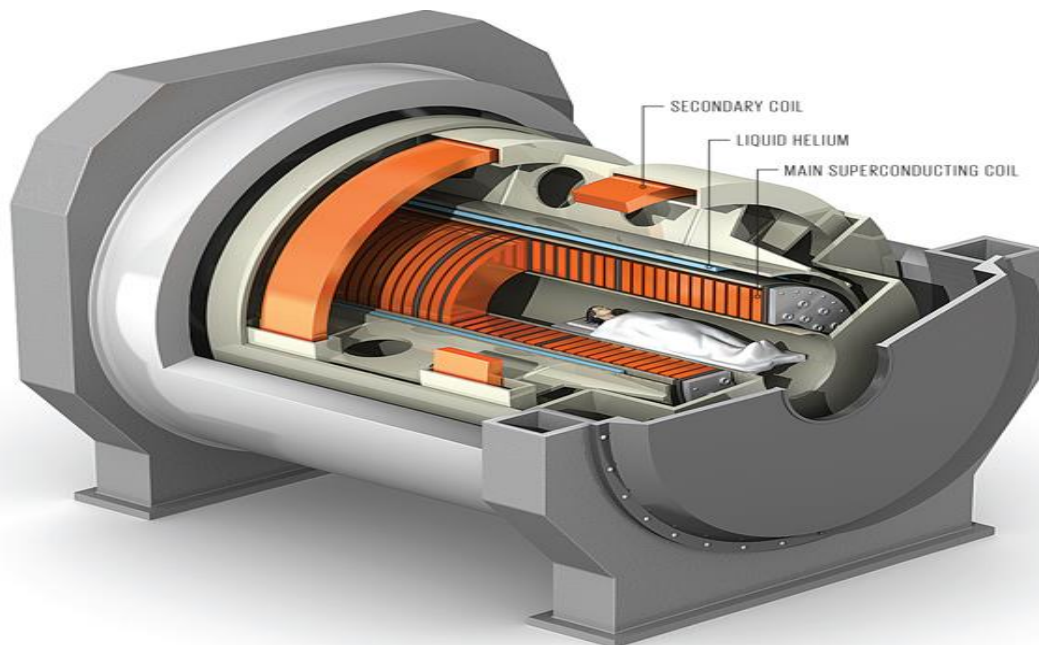
*Figure 3 -MRI Propulsion System that covers the whole frame of the body and performs imaging and targeting the Magnetic Particles at the same time (**Referenced from IEEE spectrum**).*

(c)   Main magnet.

The static magnetic field is the most important and most expensive component of an MRI system. A field strength of 1.5 T can be achieved through the use of permanent magnets. For higher field strengths, superconducting electromagnets are needed. [2]

(d)   Gradient coils.

Three gradient-coil-system arrangements are needed in an MRI system. The gradient coils are used for both propulsion and tracking. In the case of propulsion, the gradient coils generate gradient fields, which due to magnetic properties of the nanoparticles induce the actuation forces and torques that drive the nano capsules. [2, 3, 4]

(e)   Computer system.

Works as a brain of the MRI system. It connects and controls different components. It will also controls the gradient fields to provide the right amount of propulsion force for targeting and guidance.

(f)   MRI Tracking Unit

In the case of tracking, an image processing software has to work parallel with an image reconstruction software to estimate the positions and accumulation of the Nano/Micro Capsules within the vasculature, the tissues and the organs of the human. Avoiding communication delays of the image transfer and processing is the most important role of the tracking unit so the image processing part has to run as close as possible to the image generation.

(g)   System Controller _ Real-time navigation algorithm.

 The subsystem that performs endovascular navigation—can be implemented by integrating real-time navigation algorithms with the MRI propulsion system and tracking events. Optimal navigation performance requires refresh rate, duty cycle of the propulsion gradients, and repetition time of the tracking sequence. Robust controller implementation by plug-in control architectures is required to achieve automatic, stable trajectory tracking.

(h)   Graphical user interface.

In computing, graphical user interface is a type of user interface that allows users to interact with electronic devices through graphical icons and visual indicators such as secondary notation. For the implementation of a system capable of imaging and propelling the particles, the MRI interface has to be shared.
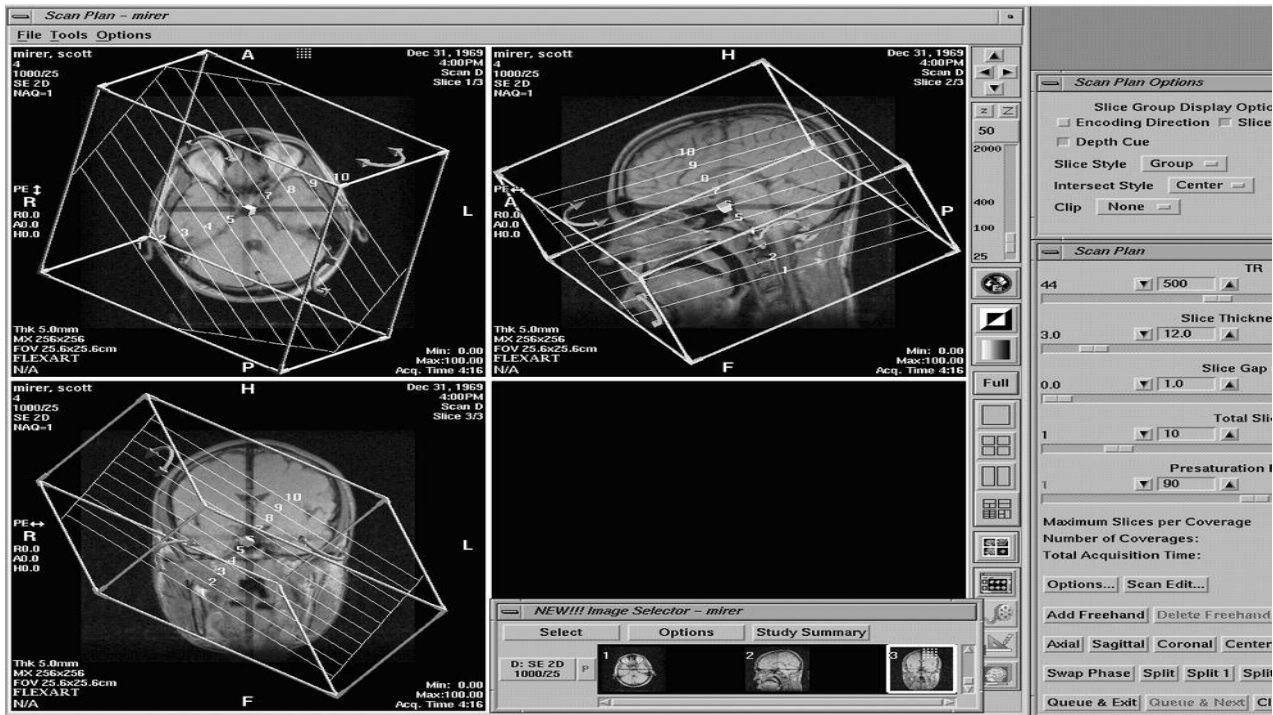

*Figure 4 Graphical user interface of a MRI showing tracking in the Brain. This system allows the user to interact with electronic devices through graphical icons and would be used as the user interface to guide and control the Particles in the human body while observing them interactively. (**Referenced from GOOGLE Image**)*

2) Dynamic Modeling Subsystem/ NANO Scale

To characterize a particle and furthermore the chain like aggregates a modeling system has been developed that contains all information of Micro/Nano particles and methods used to compute the forces acting on them. The modeling technique which can be used here is the Discrete Element Modeling (DEM). It was chosen because it provides accurate physical models for particle interactions. Figure 5 depicts the free body diagram of a single particle. Newton-Euler equations is needed to describe the principle to find the velocity and secondly the actual position of each particle in each time step regarding of the forces and moments effecting on them.

The equations are as following:

$$m_i \dot{v}_i = F_{mi} + F_{bi} + F_{esi} + F_{hi} + F_{bri} + W_i$$

$$I \dot{\Omega} = M_{hi} + T_{mi}$$

Where the index i indicates the number of particle. The linear and angular acceleration are $\dot{v}$ and $\dot{\Omega}_i$. The mass is m_i and the mass moment of inertia matrix is I . The total applied magnetics force is F_{mi}. Brownian force has been shown by F_{bri} , F_{bi} and W_i are the buoyancy and the weight forces which are negligible, F_{hi} is the hydrodynamic drag force and F_{esi} is the electrostatic

Figure 5- Free Body Diagram of a single Particle (Reference 3)

force. M_{hi} Is the hydrodynamic moment. T_{mi} Stands for the torque due to the magnetic field at the position of particle i. Be aware that it is not necessary in all the modeling simulations to involve all the forces mentioned above but optimal case would be having all gathered together in the Newton-Euler equation. Also in primary simulations as in our case as the Reynolds number of the fluid is so low the acceleration of the particles assumed to be zero. [2, 3, 4, 5, 6]

(a)   The particle module

The Particle Module methods compute the aforementioned forces based on mathematical models, which are presented in detail in the following sections. [1-7,35, 36, 37]

(i)   Magnetic forces

Due to the Micron or Nano size of the particles we can assume that the magnetic field over the

particle volume is small compared to the average field. Hence, each particle is magnetized uniformly and can be approximated by a dipole placed at the geometric center of the particle. In that case "Magnetic force" F_{mi} exerted on the i_{th} particle are given by

$$F_{m-i} = F_{dip-i} + F_{grad-i}$$

F_{grad-i}: The magnetic force due to the interaction of the i_{th} particle with the magnetic field produced in the MRI bore.

F_{dip-i}: The magnetic forces acting on the i_{th} particle due to its interaction with the surrounding magnetic particles (i.e. dipole-dipole interaction).

The force F_{grad-i} is given by:

$F_{grad-i} = (m_i.\nabla)B_{ext\_i}$

Where m_i the magnetic moment of the i_{th} particle and ∇ is the gradient operator.

B_{ext_i}: The magnetic field at the i_{th} particle generated by the superposition of the MRI superconducting magnet field and the MRI gradient coils field.

The force F_{dip-i} will be found from the following:

$F_{dip-i} = \sum_j^N F_{dip-ij}$

Where F_{dip-ij} is the magnetic force exerted on particle i due to particle j, and N is the number of the magnetic particles surrounding particle i.

$F_{dip} = -\frac{3}{4} * \frac{\mu_0\, m_i m_j}{\pi r_{ij}^4} \left(\hat{r}_{ji}\, (\hat{m}_i.\hat{m}_j) + \hat{m}_i\, (\hat{r}_{ji}.\hat{m}_j) + \hat{m}_j\, (\hat{r}_{ji}.\hat{m}_i) - 5\hat{r}_{ji}(\hat{r}_{ji}.\hat{m}_i)(\hat{r}_{ji}.\hat{m}_j) \right)$

Where μ_0 is the magnetic permeability of the surrounding medium, m_i and m_j are the magnetic moments of the i_{th} and j_{th}, particles, the symbol r_{ij} is the distance between the i_{th} and j_{th} particles, $r_{ij} = |r_{ij}|$. As mentioned above the dipolar interaction should consider all the moments effecting on each particle from the surrounding particles so the moments has to be updated in each time step and calculated for the next one using Matrix calculation.

They will be found out from the simple Matrix calculation of $m_{i-xyz} = {}^B/_A$.

B is equal to $\chi V_p H_0$ where H_o is external field, χ is the Particles Susceptibility and A is coefficient Matrix.

These Matrices has been shown for 3 particles in the following:

$$[A] = \begin{bmatrix} 1 & 0 & 0 & A(1,4) & A(1,5) & A(1,6) & A(1,7) & A(1,8) & A(1,9) \\ 0 & 1 & 0 & A(2,4) & A(2,5) & A(2,6) & A(2,7) & A(2,8) & A(2,9) \\ 0 & 0 & 1 & A(3,4) & A(3,5) & A(3,6) & A(3,7) & A(3,8) & A(3,9) \\ A(4,1) & A(4,2) & A(4,3) & 1 & 0 & 0 & A(4,7) & A(4,8) & A(4,9) \\ A(5,1) & A(5,2) & A(5,3) & 0 & 1 & 0 & A(5,7) & A(5,8) & A(5,9) \\ A(6,1) & A(6,2) & A(6,3) & 0 & 0 & 1 & A(6,7) & A(6,8) & A(6,9) \\ A(7,1) & A(7,2) & A(7,3) & A(7,4) & A(7,5) & A(7,6) & 1 & 0 & 0 \\ A(8,1) & A(8,2) & A(8,3) & A(8,4) & A(8,5) & A(8,6) & 0 & 1 & 0 \\ A(9,1) & A(9,2) & A(9,3) & A(9,4) & A(9,5) & A(9,6) & 0 & 0 & 1 \end{bmatrix} \quad [B] = \begin{bmatrix} xVpH_{0x} \\ xVpH_{0y} \\ xVpH_{0z} \\ xVpH_{0x} \\ xVpH_{0y} \\ xVpH_{0z} \\ xVpH_{0x} \\ xVpH_{0y} \\ xVpH_{0z} \end{bmatrix}$$

Three of these coefficients has been listed below to give the reader a perspective of their equations.

$$A(1,4) = \frac{-3\chi V_p}{4\pi r_{12,m}{}^5}\left(r_{12,x}{}^2 - r_{12,m}{}^2/3\right),\ A(2,4) = \frac{-3\chi V_p}{4\pi r_{12,m}{}^5} r_{12,x} r_{12,y},\ A(3,4) = \frac{-3\chi V_p}{4\pi r_{12,m}{}^5} r_{12,x} r_{12,z}$$

Where χ is the particle Susceptibility, $r_{ij,x}$ is the center to center distance of particles I and j in x direction and V_p is particle`s volume. Using the same algorithm "A" matrices can be calculated for N number of particles and used in the main Simulation platform. Meaning moments will be calculated using these Matrices in each time step and then will be implemented to the Dipolar force mentioned above for each pair of particles.

(ii)   *Fluid forces*

Due to the simple symmetry of the spherical micro-capsules, the lift, the side fluid forces and all the three fluid moments vanish. Each particle is subject only to the fluid drag force. Due to the very low Reynolds number (Re<<1) the drag force is given by the Stokes drag formula:

$$F_{hi} = 6\ \pi\eta a(v_i).$$

(a) is the particle radius. (η) is the viscosity of the blood and depends on the vessel diameter, the hematocrit of the blood and the temperature, and
(v_i) is the particle`s speed.

• Model for Hydrodynamic Interactions

So the drag force mentioned above is accurate for one particle passing through the flow, but imagine when a linear chain of particles pass the flow the number of particles in that chain has an effect on the force which each of these particles are experiencing.

There are many models that find out the drag coefficient or optimally the drag force on chainlike

particles passing through fluidic flow. In this document we consider two main models:

1. Far-Field Hydrodynamics:

Consider two interacting particles in a quiescent flow. Mobility matrix based on the notation of ''Jeffrey and Onishi, *J. Fluid Mech.* (1984)'' is:

$$\begin{pmatrix} u_1 \\ u_2 \\ \vdots \end{pmatrix} = \begin{pmatrix} a_{\alpha\alpha} & a_{\alpha\beta}\cdots \\ a_{\beta\alpha} & a_{\beta\beta}\cdots \end{pmatrix} \begin{pmatrix} F_\alpha \\ F_\beta \\ \vdots \end{pmatrix}$$

Effects of torques and stresses are neglected here. As a result matrix only includes the coefficients that relate applied forces to linear velocity:

$$a_{ij}^{\alpha\beta} = \frac{1}{6\pi\mu r_0}(x_{\alpha\beta}e_i e_j + y_{\alpha\beta}(\delta_{ij} - e_i e_j))$$

Where:

$e_i = r_i/r$

We have solved this model using Matlab and have found the drag coefficient for 2, 3 and 4 number of particles. So in simulation results section we use these coefficients for hydrodynamic force. Through researching on papers that compare this models with experimental results we concluded that this model is closer to experiments for these number of particles and seems to be matching with 2 percent error with the other model when number of particles are 200.

2. Smoluchowski (or similar)

If the chainlike rod is moving with the velocity V and it moves along the flow:

$$F = \xi_{||}V$$

$$\xi_{||} = \frac{2}{3}\frac{n}{\ln 2n - \gamma} \quad \text{Where } \gamma = 0.649$$

Comparison between these two drag coefficients has been shown on the following figure:
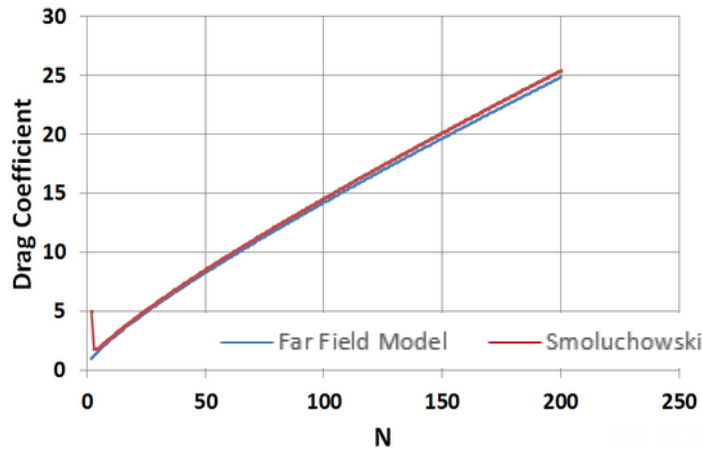

Figure 6-comparison between drag coefficients of Far-field and Smoluchowski Model-This figure shows that how these two almost match except the first 4-10 number of particles.

(iii)   Gravitational forces

The Gravitational Forces include the force due to gravity and the force due to buoyancy. Although they have limited effect at the low-end of the micro scale, they might become important when larger micron size aggregates are formulated. The gravitational force is given by:

$$F_{gi} = W_i + F_{fi} = \frac{4}{3}\pi a_i{}^3(\rho_i - \rho_f)$$

Where ρ_i, ρ_f are the density of the particle i and of the fluid respectively, and a_i is the radius of the particle i. The gravitational force can be neglected in the modeling.

(iv)   Electrostatic forces

Electrostatic force is the phenomenon that results from slow-moving or stationary electrical charges. These forces become dominant in Nano scale while they are negligible in micro scale. The total intermolecular pair potential is obtained by summing the attractive and repulsive potentials. The best known of these is the Lennard-Jones, L-J, potential:

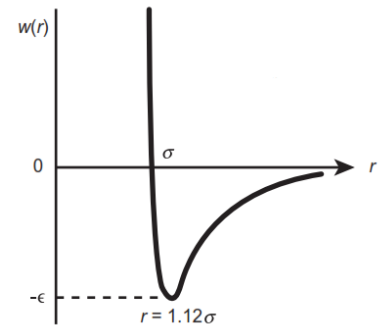$$V_{lj} = 4 * \epsilon[\left(\frac{\sigma}{r}\right)^{12} - \left(\frac{\sigma}{r}\right)^{6}]$$

Figure 7-Lennard-jones Potential (**Referenced from Wikipedia**)

Where r is the center to center distance between particles and σ is the internuclear distance. The downhill of the Lennard-jones potential is as it has the power of 12 order of magnitude in it and will have power of 13 term in force formula it can effectively slow down the process of modeling and will need smaller time steps in the order of e-13. So New model was proposed to replace Lennard_jones model. This model is an exponential force which was showing highest efficiency due to higher time steps and accurate results.

$$F_{expo} = A\, e^{k_d h_{ij}}$$

h_{ij} depicts the separation between two particles. k_d depicts 1 over the Debye length and would be a Constant but the way it is chosen would be discussed. A is also constant but it has to be somehow chosen that the particles would not jump back and forth and at the same time would not softly resolve in each other. [25]

(v)   Brownian force

Brownian diffusion effect, also referred to as molecular diffusion, becomes the dominant transport mechanism for particles less than 500 nm and is especially significant as the particles become smaller.

The Brownian random force was modeled as a Gaussian white noise process:

$$F_B = \xi\sqrt{(6\pi d_p \mu_f\, K_B T / \Delta t_s)}$$

Where $K_B = 1.38 \times 10^{-16}$ erg/K is the Boltzmann constant, T the temperature, and Δt_s the particle time step. The parameter ξ is a Gaussian random number with zero mean and unit variance.

Figure 8-Brownian motion by java simulation

To generate the white Gaussian noise the following has been used:

$$\xi = \psi\sqrt{(-2\log(S)/\,S)}$$

Where $S = \psi_1{}^2 + \psi_2{}^2$, and ψ, ψ1, ψ2 is the random number between $[-1, 1]$ and $S < 1$.

3) Experimental Validation:

As briefly explained in the introduction part of this document experiments has to be planned to validate the simulation results in different conditions and environments. For this purpose I have chosen a simple experiment on a small pipe that can be assumed to be modeling the shape of the blood vessel. Nanoparticles would be injected from one side and be guided under the magnetic field and gradients to the target. In this sample experiment if we can prove that the ratio of the particles guided to the target is close to what the simulation shows, it will validate the use of the simulation instead of the In-vivo experiments. Figure 9 shows the schematic of what one sample experiment could be.
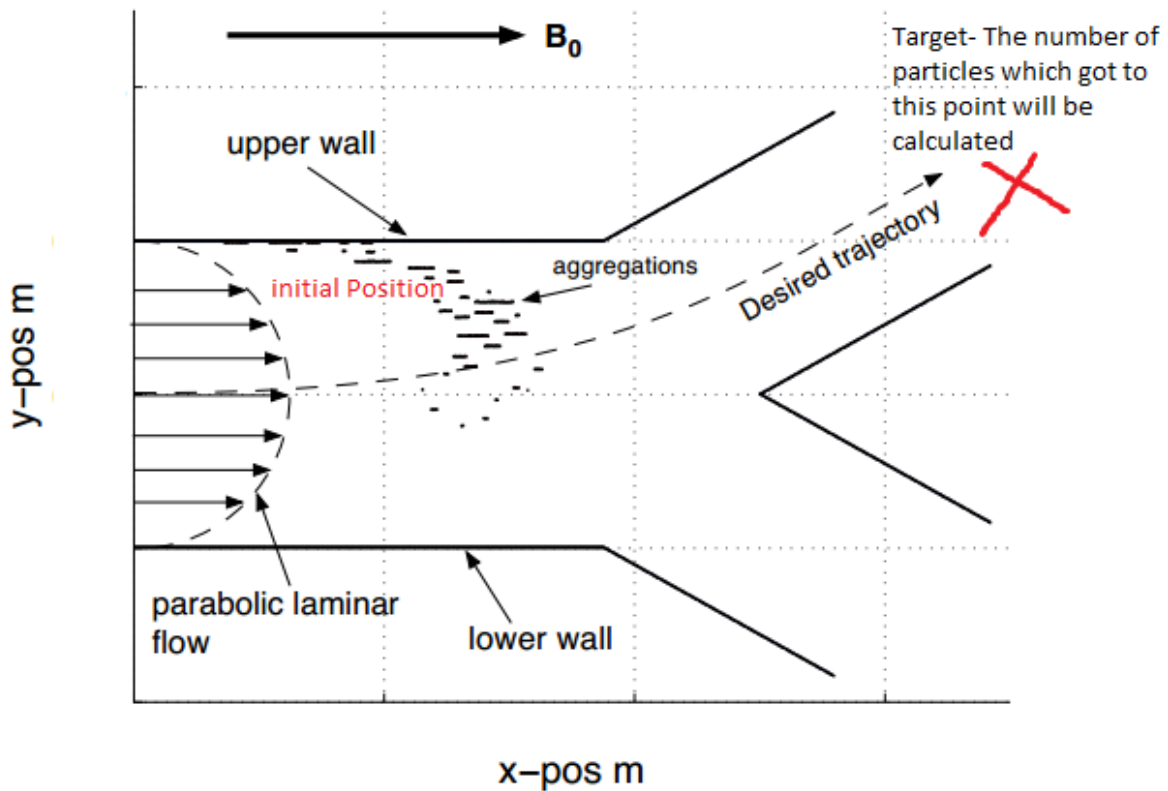

*Figure 9-The Schematic map of the ideal experiment (**Created with Paint software by myself**)*

There could be many different methods to develop the environment for this experiment. The easiest and most applicable one would be using the MRI machine with the fixed and uniform magnetic field and gradients. We would need to make or buy a phantom and set it up in the MRI machine and inject the magnetic nanoparticles from one side and observe how much of them will go to the assumed target. Phantom setup has been shown in figure 10. Using the Image processing part of the MRI machine we could be able to count how many particles have reached the target.
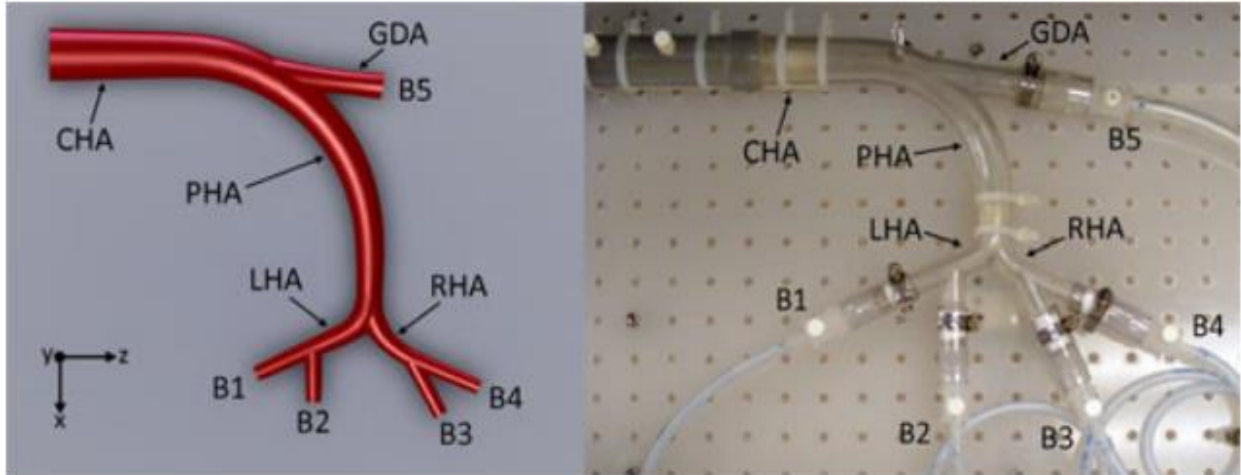

*Figure 10-Generalized hepatic artery model: (left) CAD model showing major branches and (right) photograph of 4.4×phantom model used for experiments (**Reference 32**)*

A simple Magnet also can provide the Magnetic Field and Gradients, It would be just harder to find an optimum condition that these fields are uniform. The magnetic flux coming out of the magnet will vary by distance so we have to find a really small scale experimental environment that can demonstrate the uniform field and gradients. Fig 11 shows the schematic of this method of experiment. The magnet and the pipe can be seen in the picture. Beside, Gauss meter and square cross section glass capillaries can be beneficial.

*Figure 11 -Schematic of A Magnet Propulsion experiment (**Picture took in DAPS Laboratory**)*

Ideally in my point of view is very beneficial to make a device that is similar to the structure of the MRI machine and enables us to provide Magnetic Field and gradients and let us control them the way needed. Motion experiments of super paramagnetic nanoparticles require: (i) the presence of a uniform magnetic field for magnetizing the nanoparticles and (ii) the presence of a variable magnetic gradient for controlling the magnetic force acting on the magnetized nanoparticles. The uniform magnetic field can be generated by a pair of Helmholtz coils. The linear magnetic gradient can be generated by a pair of Maxwell coils.

A schematic of the pair of Maxwell coils is depicted in Figure 12. The magnetic field B_{M_z} along the symmetry axis of the Maxwell coils is given by Equations. The resulting field within the workspace is a constant magnetic gradient. A schematic of the pair of Helmholtz coils is also shown in Figure 12. The current flowing in the coils has equal magnitude and same direction. The resulting magnetic field within the workspace is almost constant and uniform.
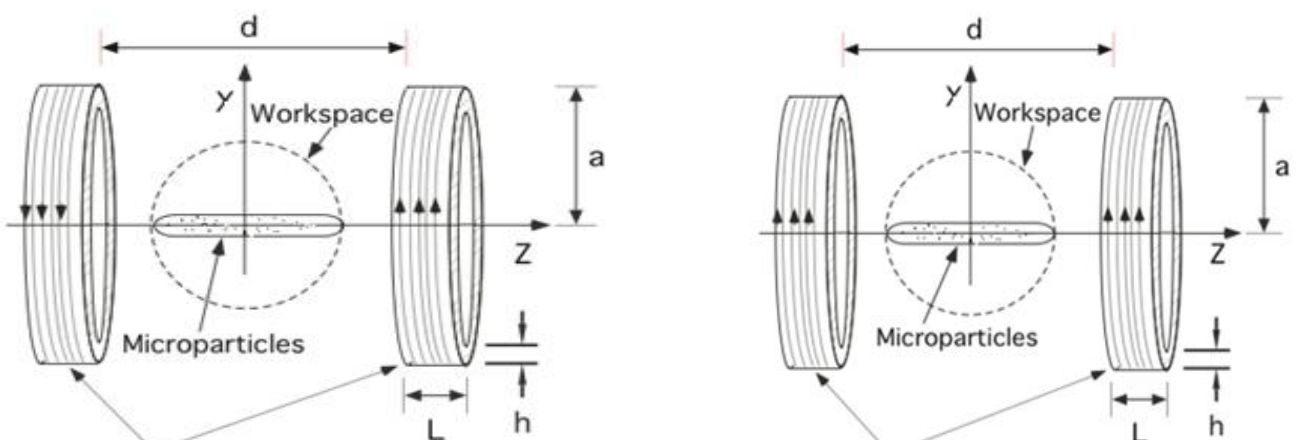

*Figure 12-(LEFT) Pair of Maxwell coils, (RIGHT) Pair of Helmholtz coils (**Picture Made in BML group**)*

Each Maxwell coil is placed inside a Helmholtz coil. The final coil configuration is depicted in Figure 13 which depicts the coil set up including the bobbins of the coils and the plastic support that fixes the coils onto the base of the set-up. In Figure 14 the complete coil setup including the microscope can be seen.
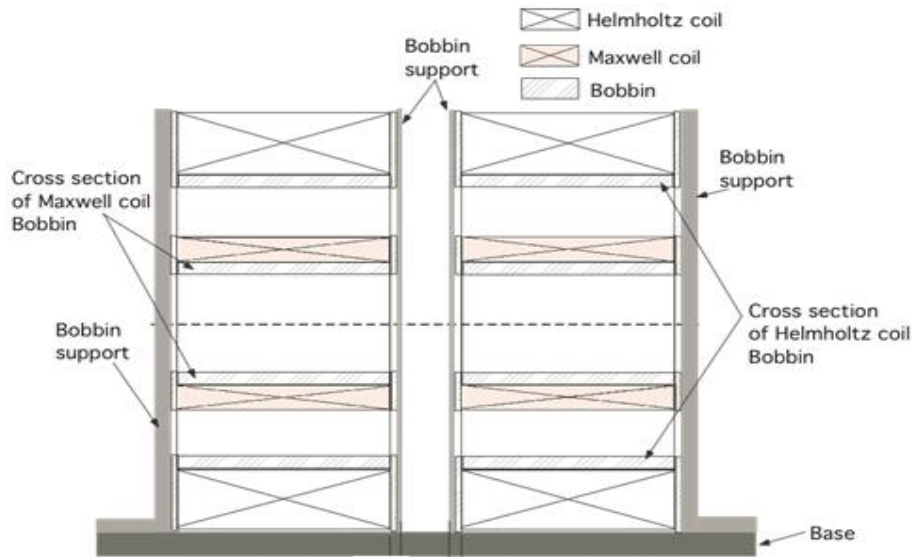

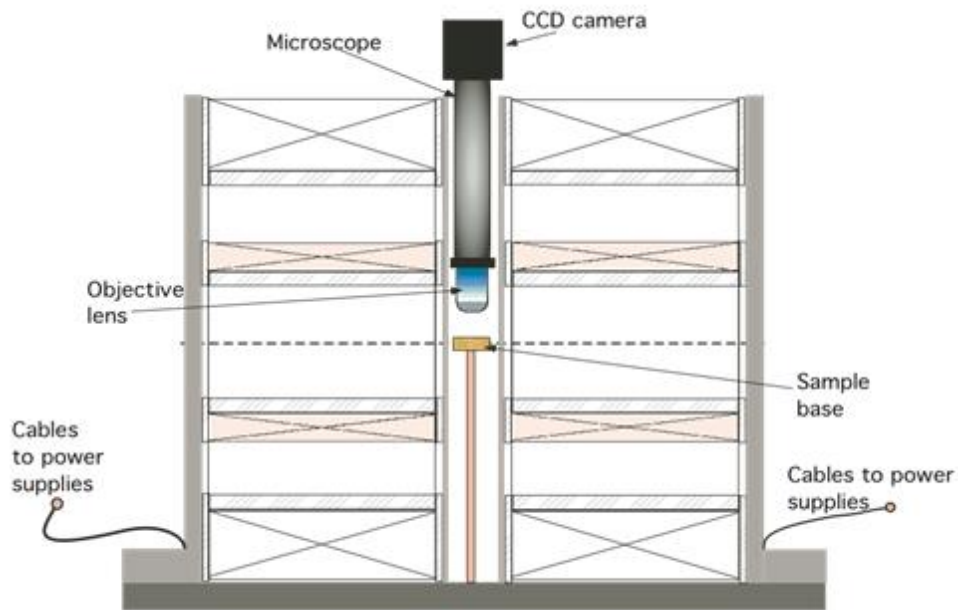*Figure 13-Coil set-up including bobbins, plastic supports and base.*

Figure 14-depicts the complete experimental set-up including the microscope

The CAD design of the complete coil set-up (including the external plastic supports and the base) was built using the Solid works. Figure 15.A shows the 3D CAD drawing of the left set of coils. The set of coils is supported from one side by a plastic plate, the other side is not covered by a plate for demonstration purposes. Figure 15.B shows the same set of coils enclosed by the two lateral supports and the base. Finally Figure 15.C depicts the complete 3D CAD design and Figure 15.D its lateral cross-section.
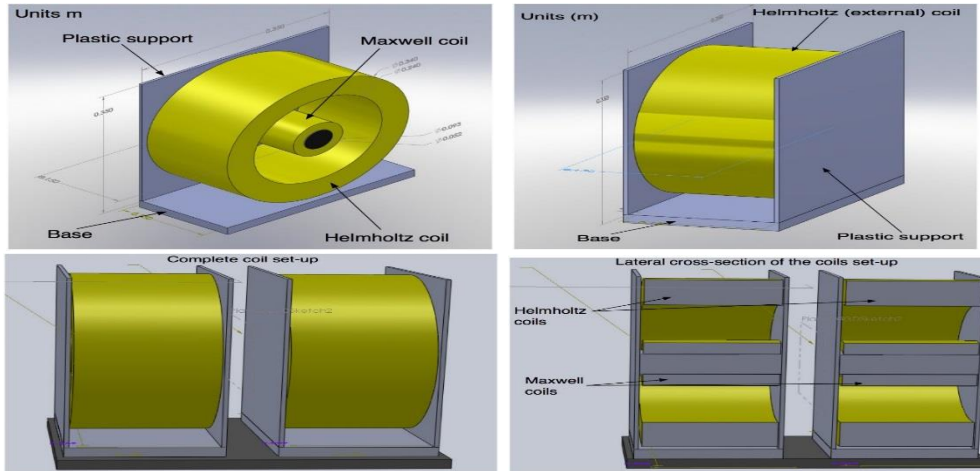

Figure 15-Angle view of one set of coils. The external coil is the Helmholtz coil and the internal is the Maxwell coil, B) Angle view of one set of coils. The coils are supported by two lateral plastic supports and a plastic base, C) 3D CAD design of the complete coil setup, D) Lateral cross section of the coils set-

The sample that has to be used to go under the microscope can be a simple channel that can be just two slides on each other and the fluid trapped in between but at some point it has to be improved to a capillaries as similar as to the real ones in human body. These capillaries would be modeled and 3Dprinted to be the sample of the experiments. By modeling them in couple of angles, Sizes and cross Sections, huge amount of data for control and guiding nanoparticles would be generated to be compared by computational platform. Figure 16 shows a sample microfluidic channel that has been designed and printed by us. PDMS is a substance that can be used instead of 3D Printing. Transparency is the benefit of this method since the microscope visualization would be much higher than 3D printed materials.
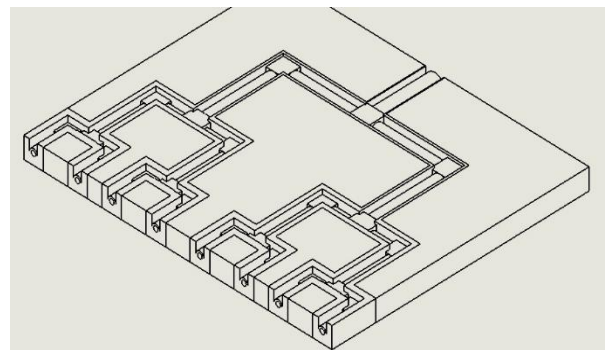
Figure 16-Sample of microfluidic channels, designed followed by Murray`s Law.

Our experimental setup that has been perform in DAPS lab is close to the setup that has been shown above as the ideal setup(Figure 14) and only difference is the Maxwell and Helmholtz coils have been replaced by solenoids but still the effect of the Fixed magnetic field and the gradients is there. Figure 17 shows this setup while the results that been observed will be shown in the result section of this document.

Figure 17-The setup performed in DAPS lab using microscope, solenoids, microfluidic channels And Audrino

V.Simulation Results:

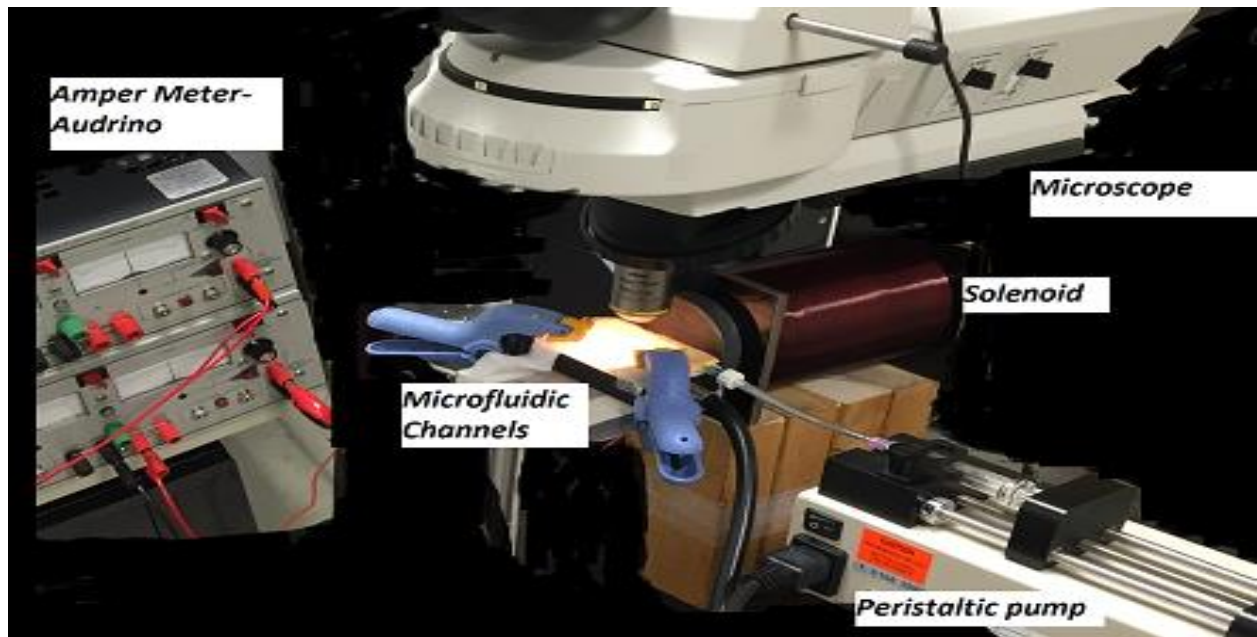First I want to say that the modeling started with just creating 3 particles aligned in advance. We started from the micro scale showing that how a system that has been effected by the magnetic field, gradients, Magnetic dipolar interaction and A spring system as the steric force would react. We intentionally did not consider the Brownian force so we would find out the noise and perturbation effects only caused by the spring force. For this analysis first we had to find out the optimum spring constant that would create harmonic interaction between particles not pushing them far away or softly attach them together.

This analysis was performed using MATLAB for two particles with 2.8 micron size and gradient was parallel to X axis equal to 0.3978 T/m and the field is parallel to X axis equal to 100 Gauss.

-4	0.000112
-3	0.000112
-2	0.000112
-1	0.000228
0	0.001017
1	4.21E-04
2	0.000123
3	0.000317
4	0.002158
5	0.020569
6	0.204682
7	2.045806
8	20.45705
9	204.5695
10	2045.694
11	20456.94
12	204569.4
13	2045694
14	20456939

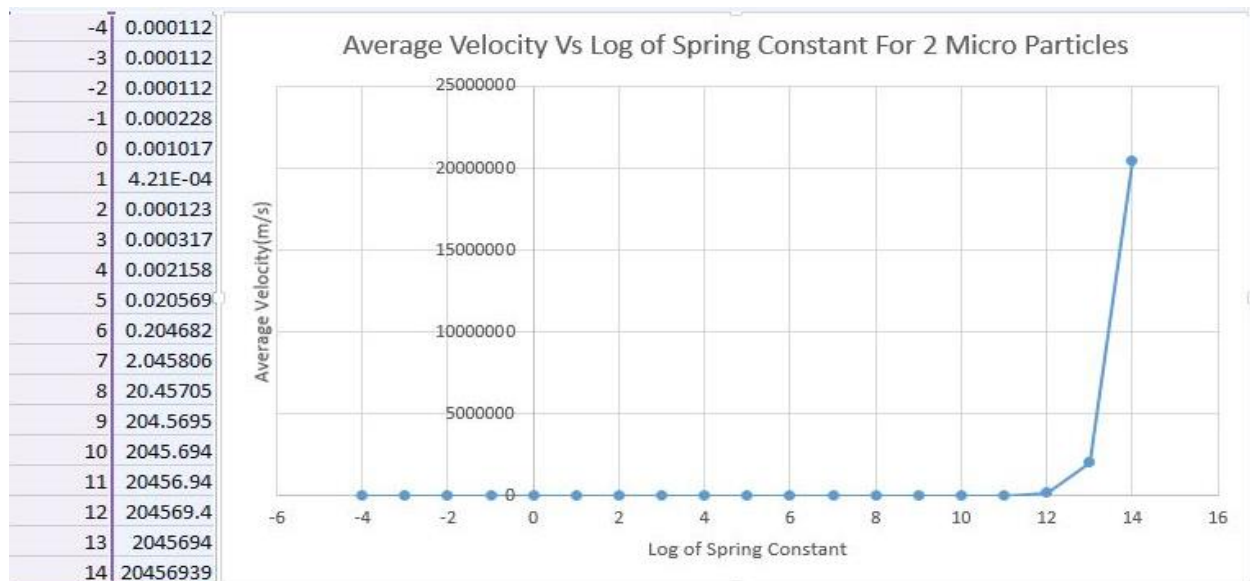*Figure 18-Average Velocity Vs Log of Spring Constant for 2 micro particles*

As it is shown in figure 18 the velocity stabilize when logarithm of spring constant varies from -4 to 12 and it gets noisy when it gets more than 12. So a good choice for spring constant can be e-4. For the reader to be more able to see the stabilizing of the movement the zoomed figure of the above figure has been shown in the following.
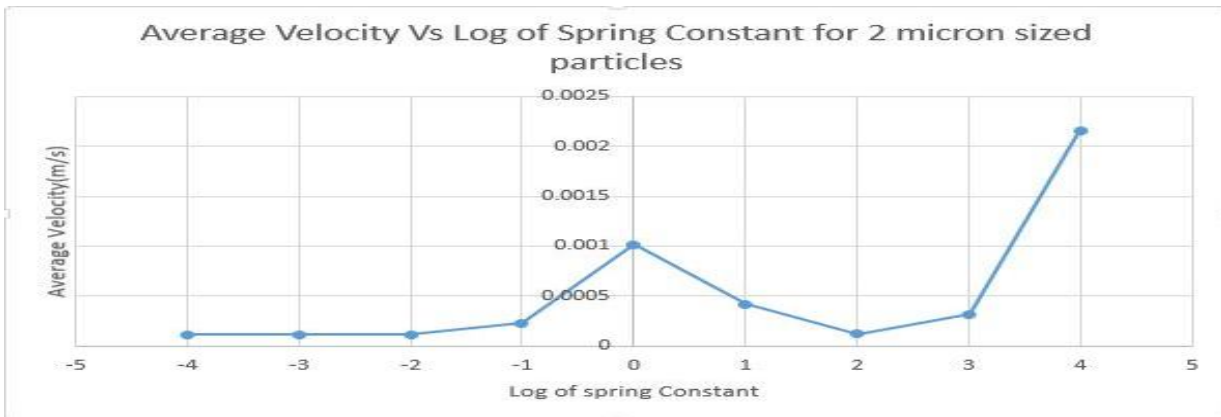
In the above figure it is obvious how the velocity stabilize in the spring constant range of 1e-4 to 1e-1 so basically this range would be reasonable to choose the spring constant.

While the spring model was tested in micro scale, we tried this same model in Nano scale to find the noise regime and perturbation in this scale as well.

Two 75nm particles aligned in advance has been put under the magnetic field equal to 100 gauss and the gradient is parallel to X axis equal to 1.88 T/m. Same as Micro scale We intentionally did not consider the Brownian force so we could find out the noise and perturbation effects only caused by the spring force. For this analysis Mutual induction has been included as well.

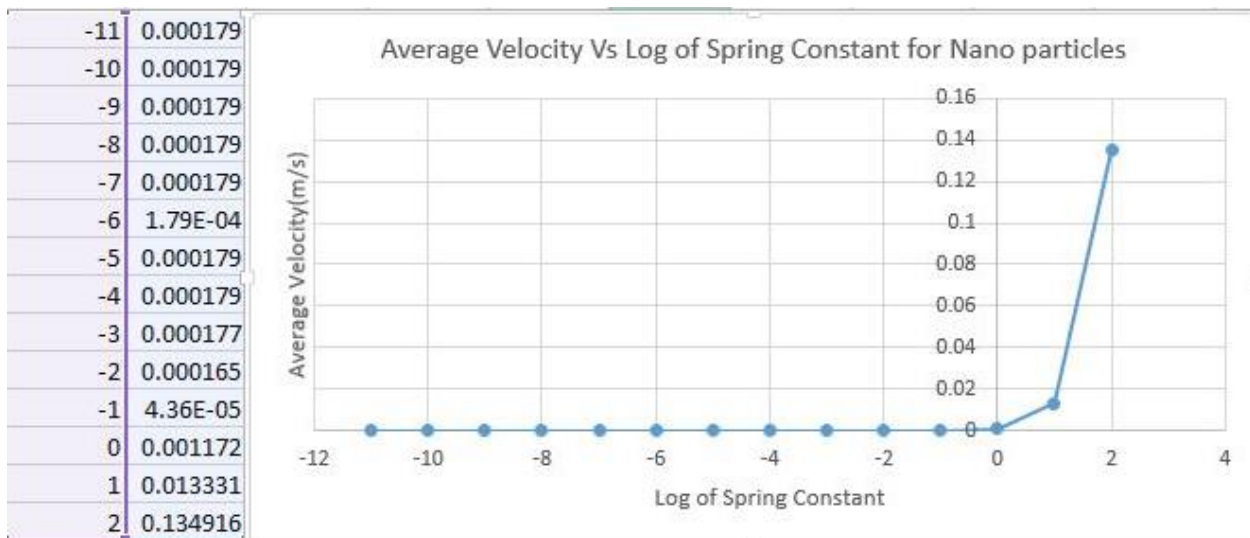|	
-11	0.000179
-10	0.000179
-9	0.000179
-8	0.000179
-7	0.000179
-6	1.79E-04
-5	0.000179
-4	0.000179
-3	0.000177
-2	0.000165
-1	4.36E-05
0	0.001172
1	0.013331
2	0.134916

Figure 19-Average Velocity Vs Log of spring Constant for Nano particles- It gets noisy when spring constant goes higher than 1.

As it can be seen in the Figure 19 the particles tend to get noisy when spring constant goes higher than 1 and they seems to have high stability in the range of 1e-11 to 1e-7 which gives us the range that would be proper to choose the spring constant from.

Well, as mentioned before the spring model is not realistic and there should be a model which is closer to the concept of an electrostatic force like Lennard_Jones. So we came up with one exponential model to replace this steric force and from now on I call it expo model in this documents. The following formula has been used to describe the Exponential force.

h_{ij} depicts the separation between two particles. k_d depicts 1 over the Debye length and would be a Constant but the way it is chosen would be discussed. A is also constant but it has to be somehow chosen that the particles would not jump back and forth that much and at the same time would not softly resolve in each other.

$$F_{expo} = A \, e^{k_d h_{ij}}$$

To find out the optimum proper A and k_d Professor Erb proposed to compare the exponential force with the magnetic force in the case that particles are aligned and magnetic field is parallel to alignment direction and no mutual induction is included. The goal is to find out by which A and k_d their figures will match better. We started in Micro scale and k_d is constant equal to 1/400e-9. From the following Figure we could get an estimate that A would better be between 1e-10 and 1.6e-10.
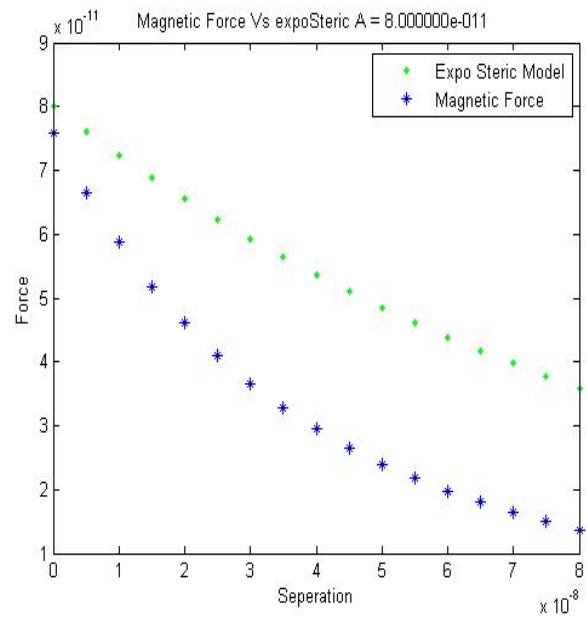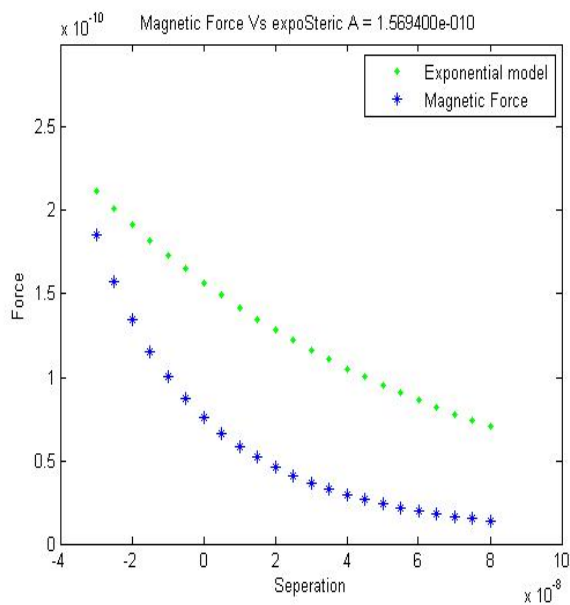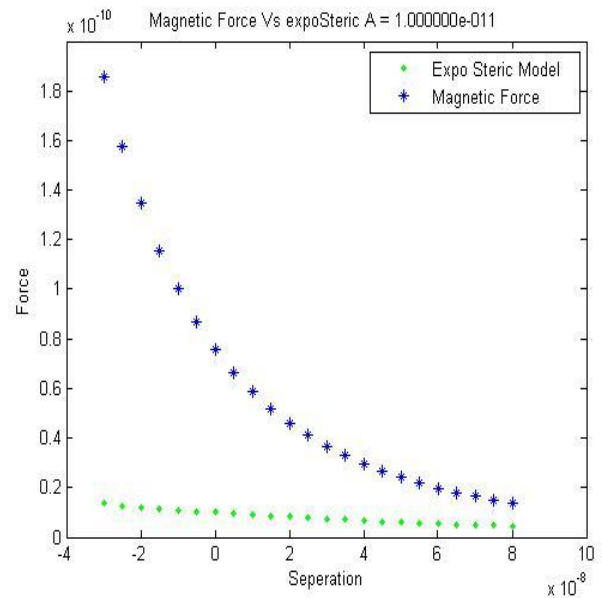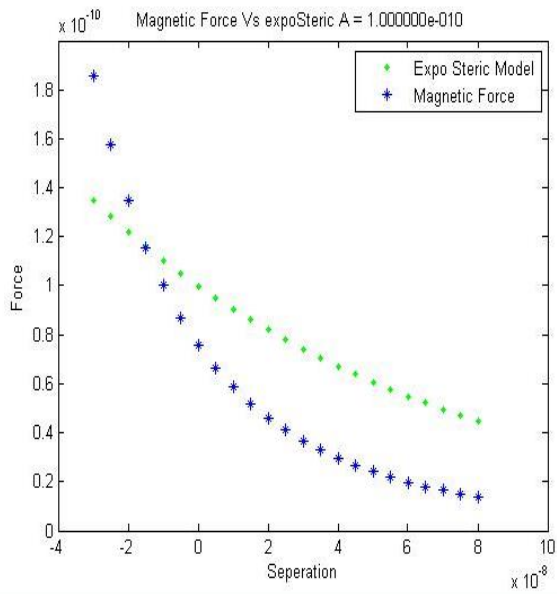
Figure 20- Comparing steric model and Magnetic force to find an optimum A constant- Different parameters for A, k_d has been plotted to show how Magnetic Force will change with Exponential model to find the perfect match of them finding Optimum A, k_d

While this comparison was giving us a good insight of how to find the A constant of this force formula, Professor Erb came up with a new idea which was to match the total force of Magnetic and the Expo steric and compare that to the shape that Lennard Jones Force has to have.

Figure 21-Total Force (Magnetic + Steric) Vs separation Nano scale

Figure 22-Total Force (Magnetic + Steric) Vs separation Micro scale

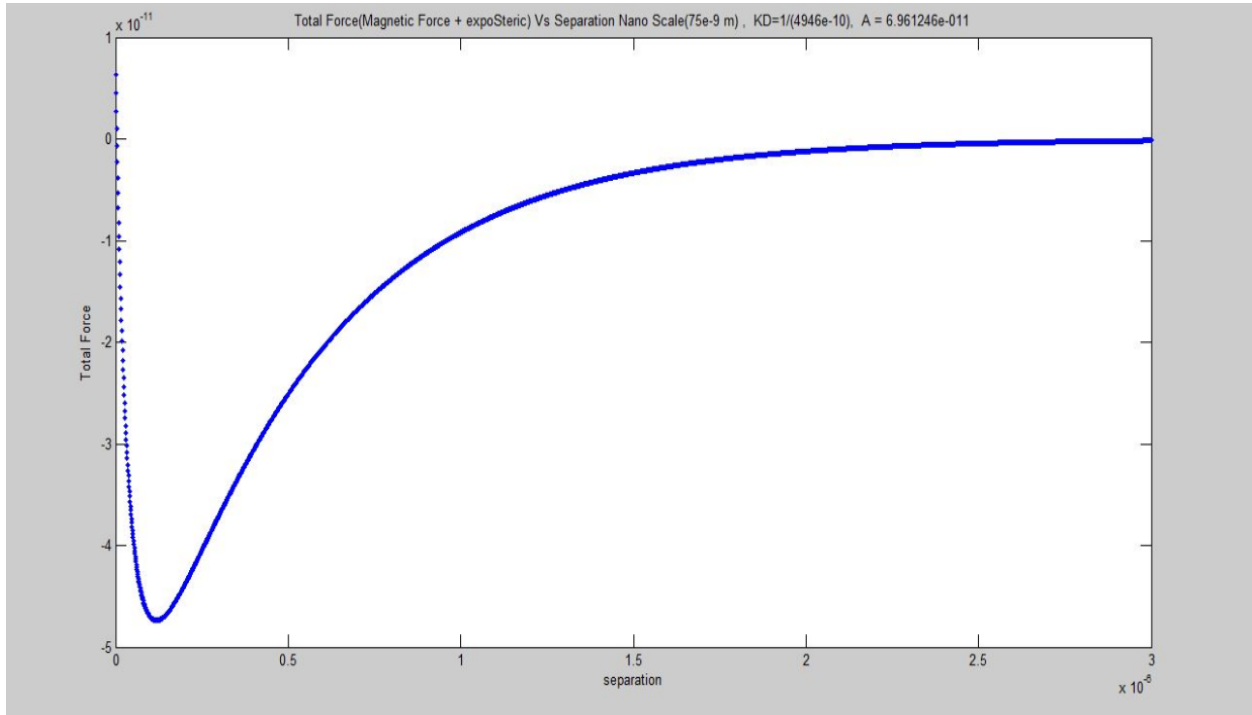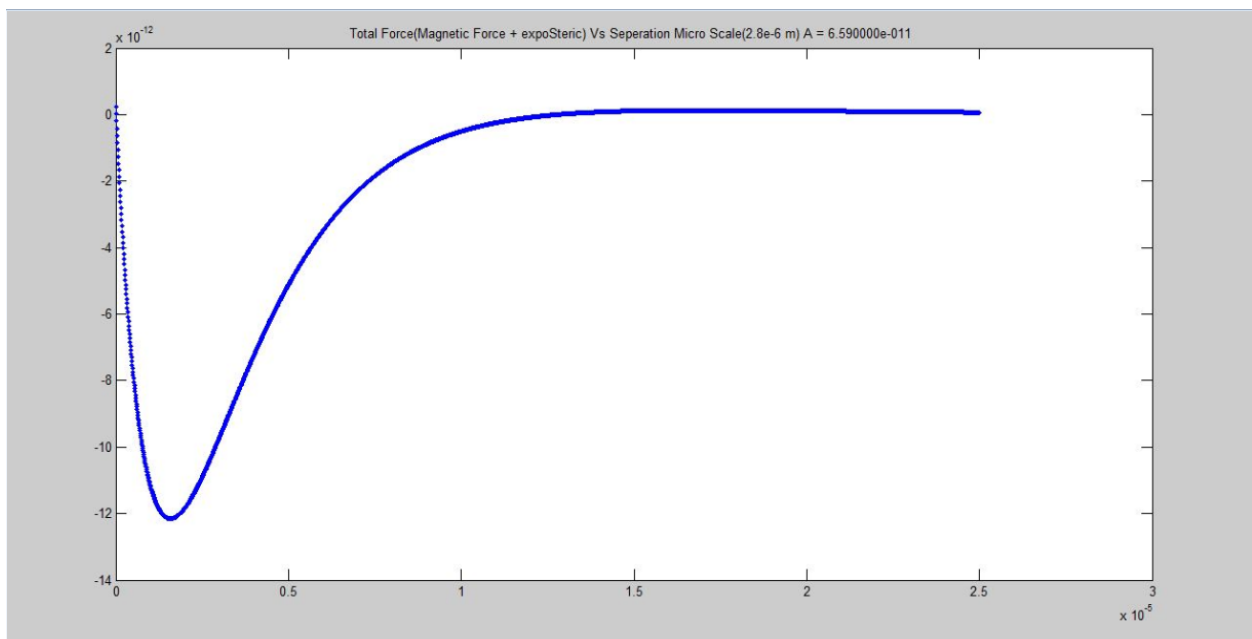Well, the above figures show how the total force matched the desired figure of Lennard jones force. So by these figures for the specific size and gradients that mentioned we could implement these A and k_d to the exponential steric force model and run the simulation. The key point is how to choose these values so we get the desired equilibrium distance between the particles in chains. Meaning we can assign A and k_d somehow that the particles softly touch and push on to each other or they keep away from each other by a distance. We have done simulations for 1 micron sized diameter particles, 2.8 micron sized diameter particles and 150 nanometer sized diameter particles. The reason is we have these particles in our research Lab so we are able to experimentally model them and validate our simulations, which was what we did.

For all the following experiments we have assigned A, k_d values as the particles stay put as a chain with a distance of 10 to 20 nano meters that gives us a better chance of getting uniform average velocity through the whole duration of particles movement.

The main properties of them which changes by size is Susceptibility of theirs which is 4.1 in Nano and goes to 0.41 for 2.8um size particles. The fluid viscosity is 0.0025 Pa.S and the magnetic permeability of the surrounding medium is 4πe-7.

We primary did simulations for 1, 2, 3 and 4 number of particles in 2 different case. With and without mutual induction. Simulations performed with fixed gradients and changing field.

The magnetic field which has been assigned parallel to X Axis is changing from 100 gauss to 500 gauss. And the fixed gradient is also parallel to X axis and it is 1.6 T/m.
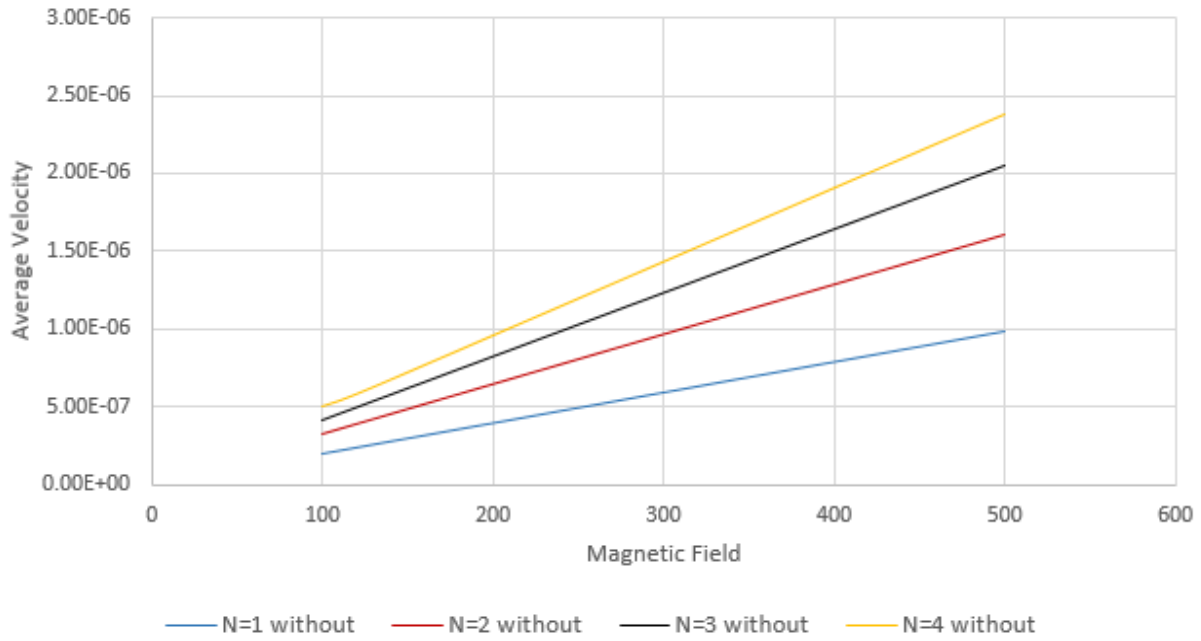
A. One micron

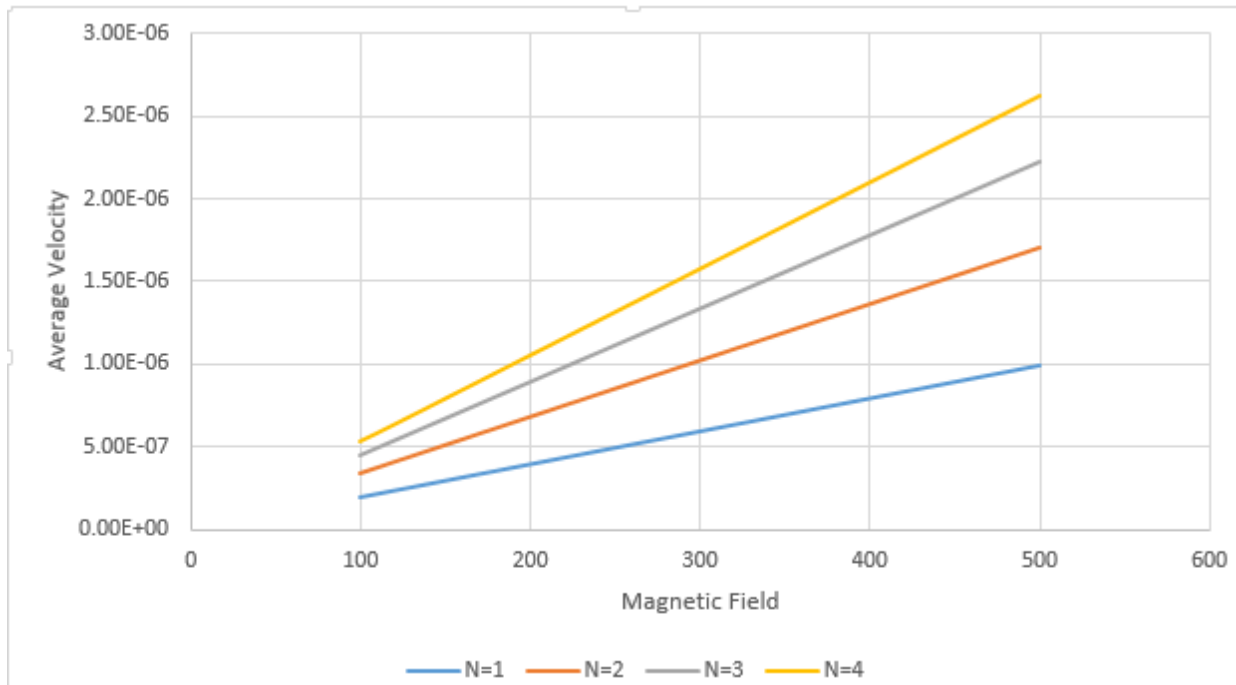*Figure 23- 1 micron particles without Mutual Induction*

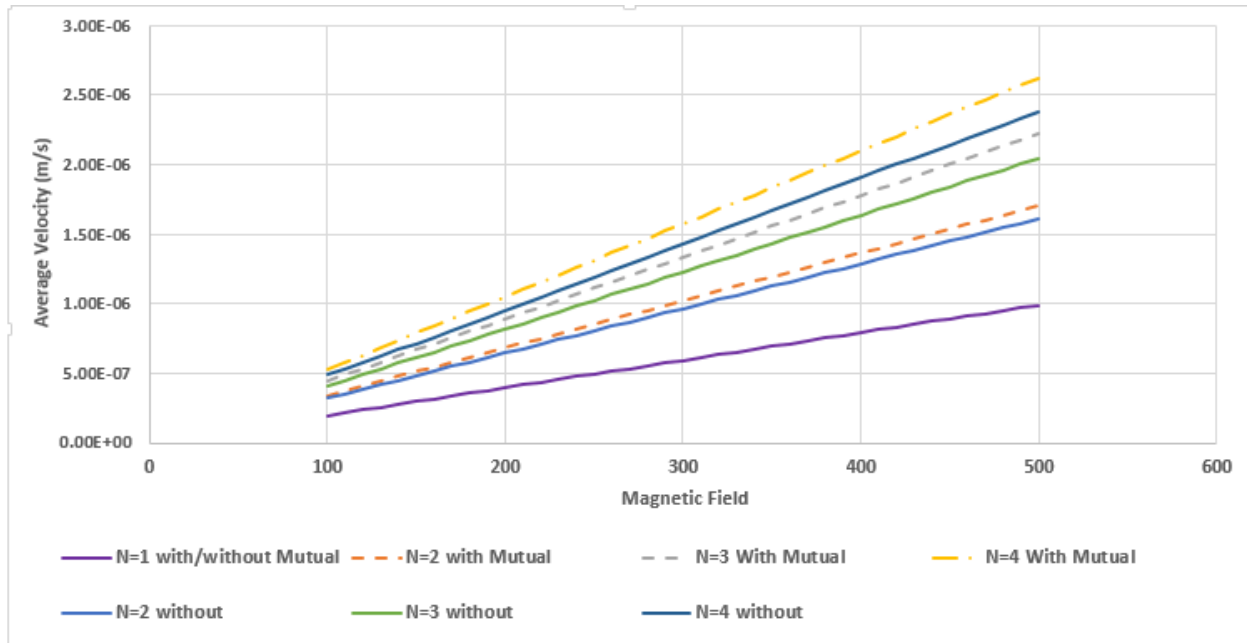*Figure 24- 1 micron particles with Mutual Induction*

Figure 25 – 1 micron Particles with and without Mutual induction- Dashed Lines are without Mutual induction

So the above figures show the average velocity of Particle chains versus the magnetic field. The first clear conclusion of the figures is that the average velocity increase when the number of particles in chains increase. The average velocity increases when the magnetic field goes up. The other important thing is in chains with same number of particles the one that is being included of the Mutual induction moves faster than just a simple moment without including the mutual moment induction in between particles. The other important thing that might a clever mind ask is what do we mean by chains? Meaning how are we chaining the particles? Do they collide? Do they just touch or they keep a specific distance? And it is interesting that in each of these options the average velocity of the chain would be different. So the one that we chose is we tend to make the steric force somehow that the particles keep a specific distance from each other as in real case they also are being separated by a specific distance due to the ligands that is attached to the surface of particles. The average distance for each case of the simulations above have been shown in the following Table.

Table 1-Average Distance For different number of particle chains with and without mutual induction

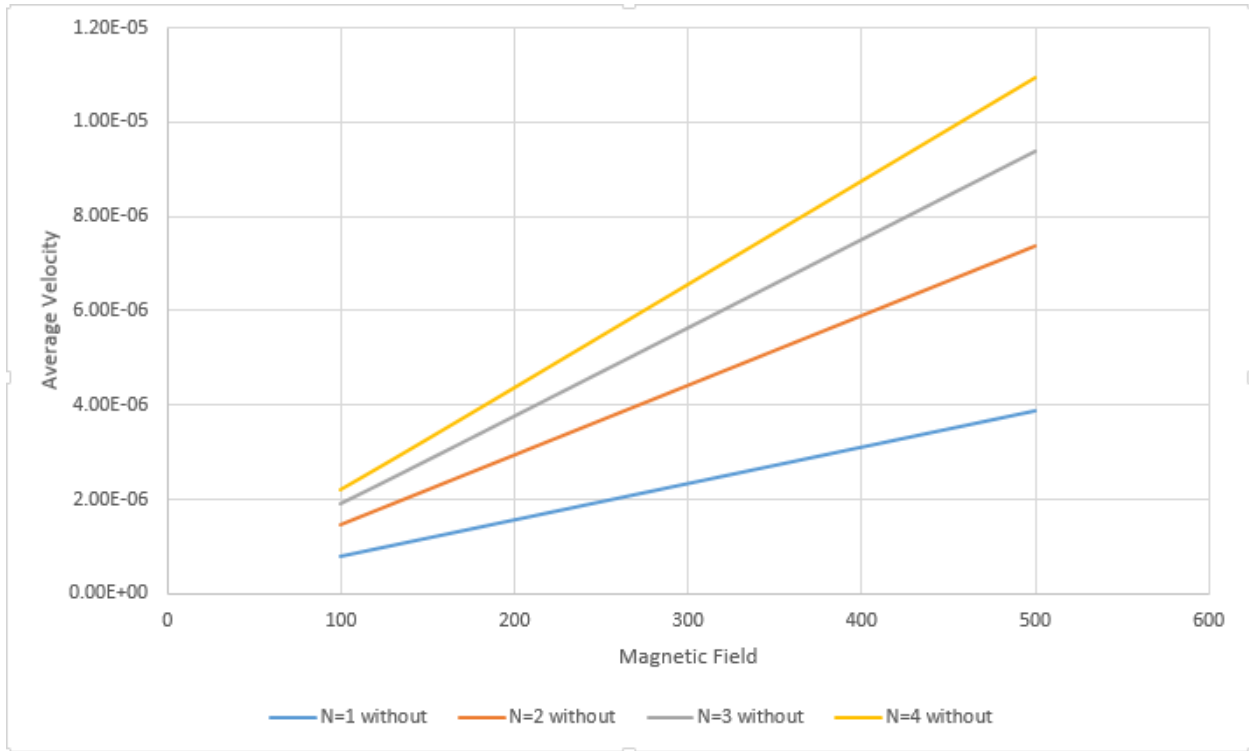|	Average Distance(m) N=2	Average Distance(m) N=3	Average Distance (m) N=4
Without Mutual	1.04E-08	1.44E-08	1.31E-08
With Mutual	1.01E-08	1.22E-08	1.52E-08

B. Two point Eight Micron

Figure 26- 2.8 micron particles without Mutual Induction
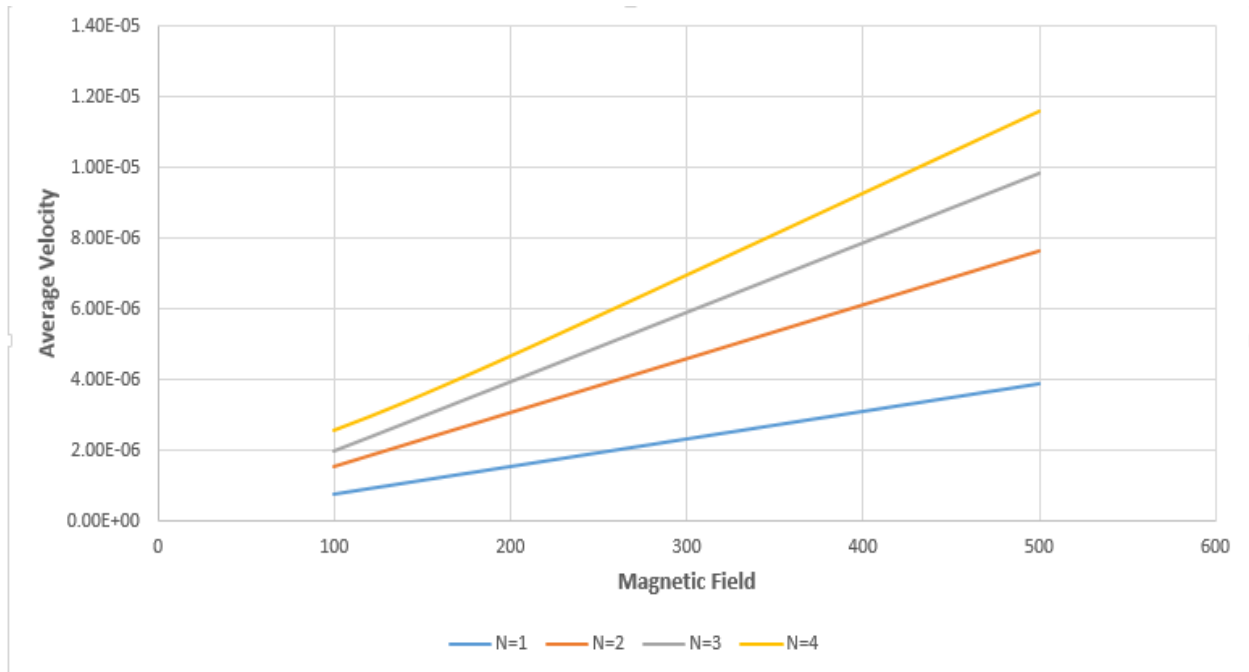
Figure 27- 2.8 micron particles with Mutual Induction
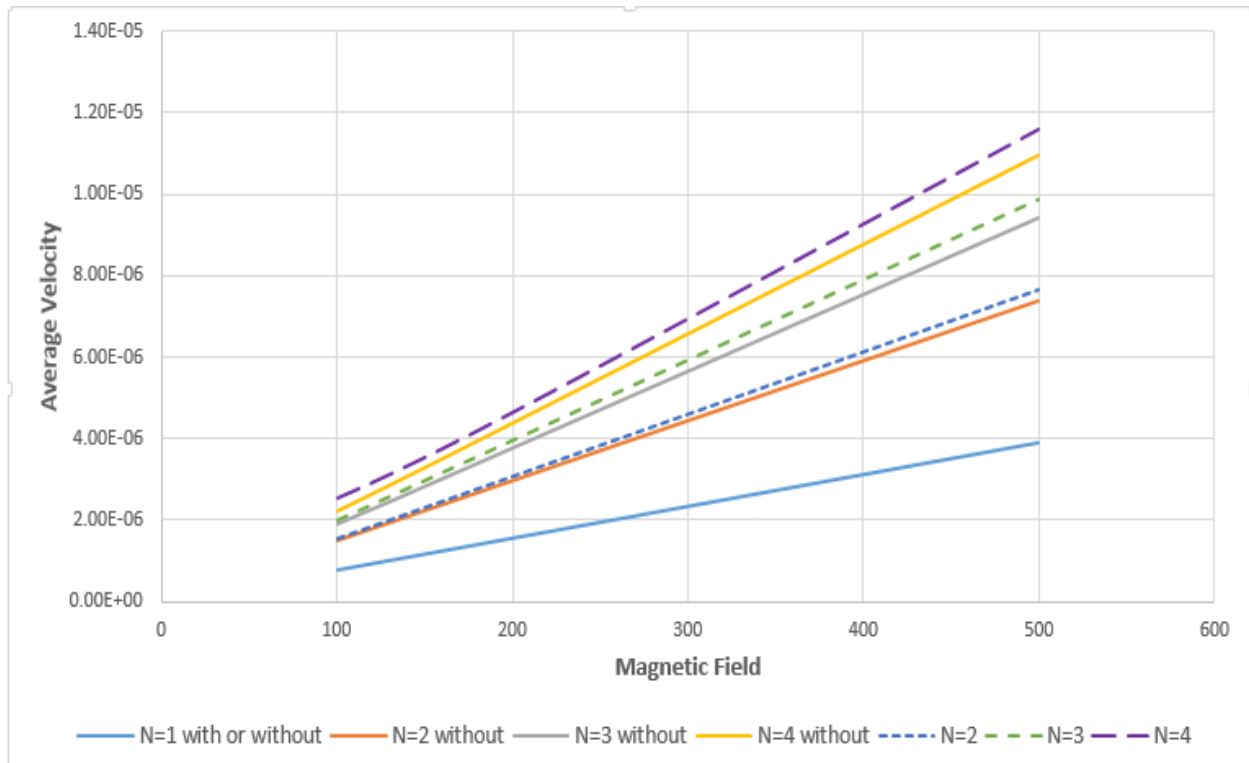
Figure 28 – 2.8 micron Particles with and without Mutual induction- Dashed Lines are without Mutual induction

So from the above figures we can get the same conclusion as of 1 micron particles:

- Average velocity increase when the number of particles in chains increase.
- Average velocity increases when the magnetic field goes up.
- In chains with same number of particles the one that is being included of the Mutual induction moves faster than just a simple moment without including the mutual moment induction in between particles.

As we did for 1 micron particles the average distance for each case of the simulations above have been shown in the following Table.

Table 2- Average Distance For different number of particle chains with and without mutual induction

	Average Distance(m) N=2	Average Distance(m) N=3	Average Distance (m) N=4
Without Mutual	1.66072E-08	1.66E-08	1.50E-08
With Mutual	1.79E-08	1.62E-08	1.75E-08

C. Hundred fifty Nano Meter

Figure 29 – 150 nm particles without Mutual Induction
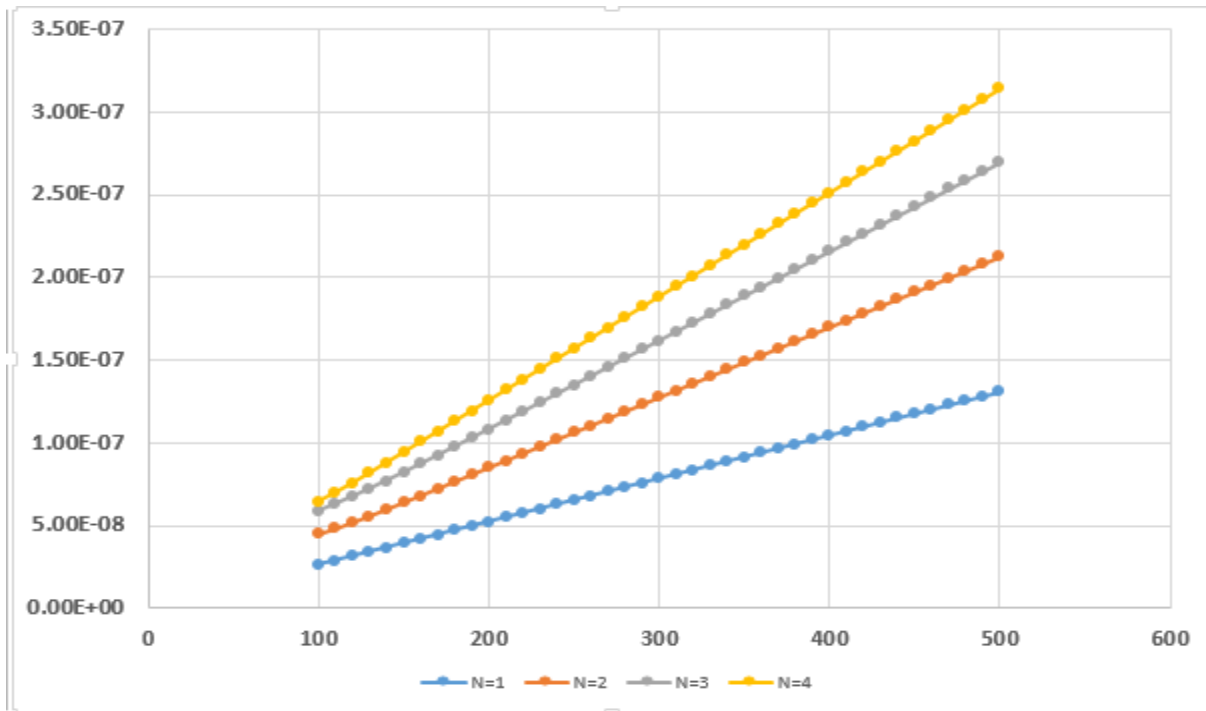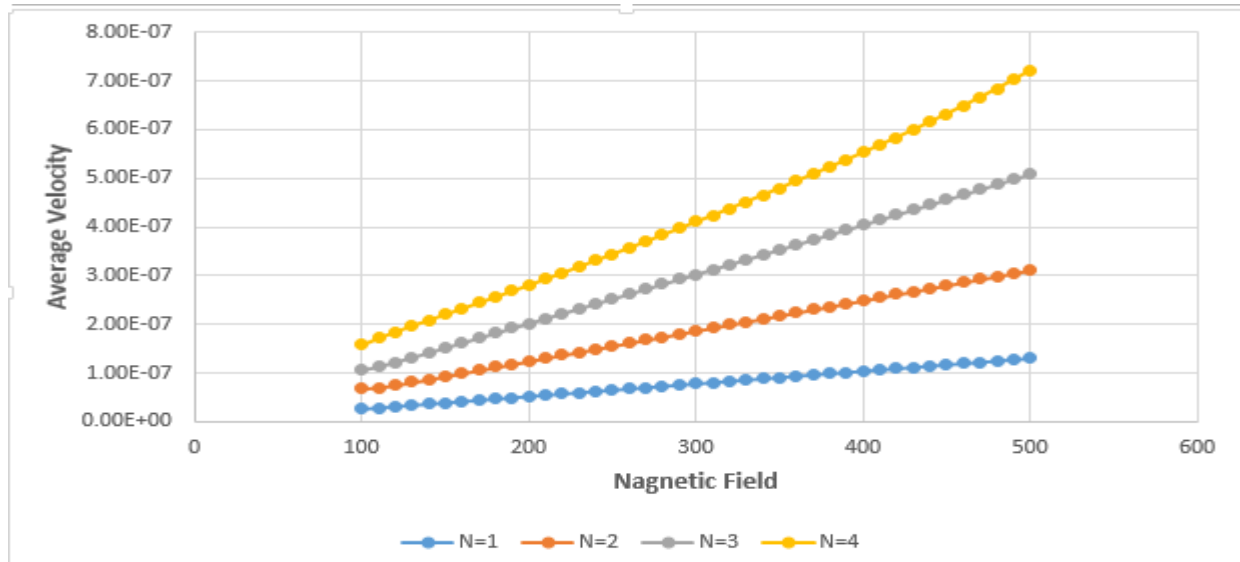

Figure 30 - 150 Nano meters particles with Mutual Induction
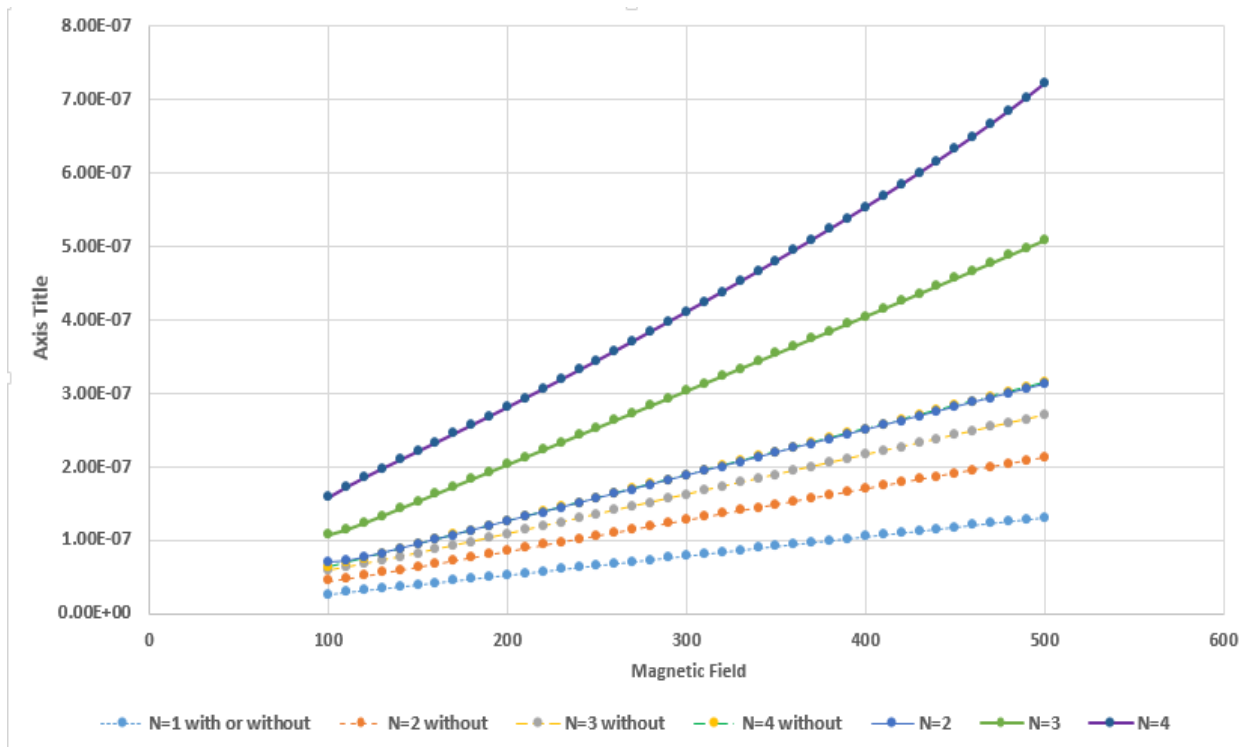
Figure 31- 150 Nano meter Particles with and without Mutual induction- Dashed Lines are without Mutual induction

Table 3-Average Distance For different number of particle chains with and without mutual induction

	Average Distance(m) N=2	Average Distance(m) N=3	Average Distance (m) N=4
Without Mutual	4.71517E-09	3.64358E-09	1.10985E-09
With Mutual	3.16112E-09	3.08037E-09	3.6882E-09

Nano scale results has been compared in figure 31 for average velocity of different number of particles with and without mutual induction. Nano results with mutual induction all were higher than the ones without mutual induction meaning 2 number of particles with mutual induction included have almost the same velocity as 4 particle chains without mutual induction. This shows that mutual induction has much higher effect in Nano scale rather than the Micro and the velocity enhancement is more in Nano scale.

Still as the number of particles in chain increase the average velocity of the chain increases as well. These primary results were all gained without taking into account the Brownian motion of particles. It should also be mentioned that the average distance between the particles which is relatively being controlled by A and k_d values of steric force has a high impact on this velocities.

To add the Brownian Force to the simulation we need to figure out how long the simulations should be running before we can stop them and find the average velocity of the chains.

So we ran some simulations in advance to find out what would be the desire simulation time in Micro and Nano that the average velocity converge to a constant time so that value could be used as the Average Velocity of chains including Brownian motion.
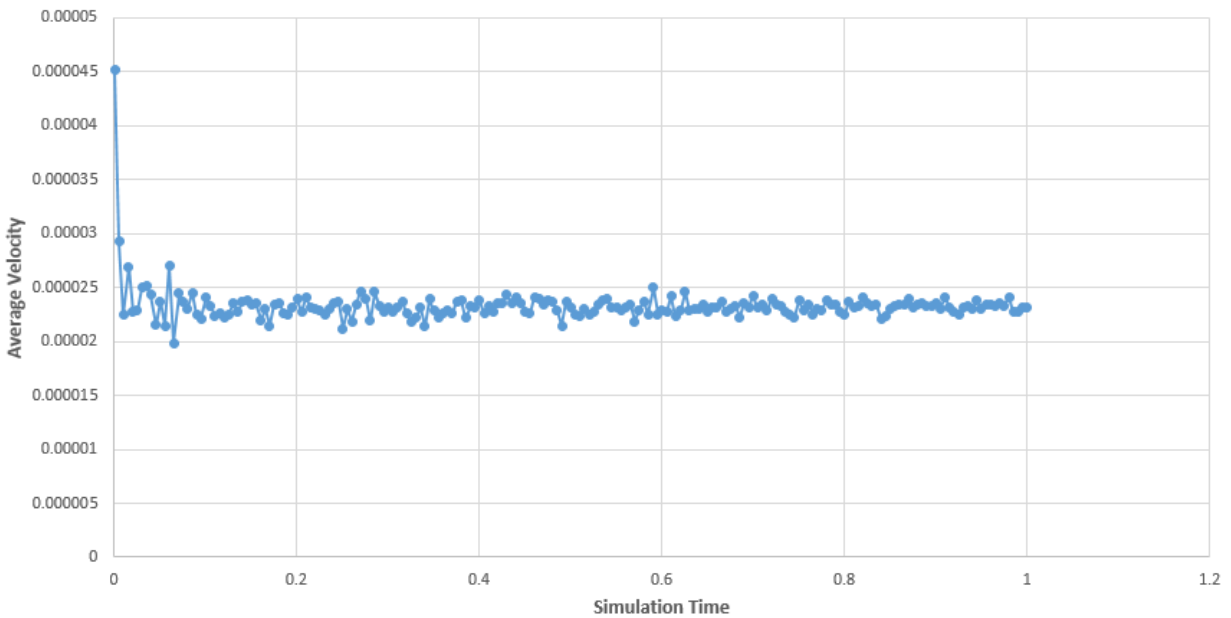
Figure 32 - one particle of 2 micron diameter- Average Velocity Vs Simulation Time including Brownian Force

Figure 32 shows one particle of 2 micron size diameters average velocity versus the simulation time as it can be seen the average velocity seems to converge as simulation time increase so for lower simulation time noisy behavior of average velocity can be seen while the simulation time gets to almost 0.7 second the standard deviation of the velocities is much lower and almost converging to 2.3e-5 m/s which is close to without Brownian motion results for 1 particle showing the Brownian motion is not dominant in Micro scale. The same simulation has been done for 2 particles of 2 micron size. For 2 particles we also take into account that their behavior would be different if particles were staying aligned by a constant distance in between or colliding to each other on a certain range. Figure 33 shows average velocity versus simulation time for 2 particles overlapping in the range of 10 to 20 nano meters during simulation time while Figure 34 is the same without overlapping as the particles stand by each other with at-least 20 nanometers distance.

In both cases the converging simulation time is around 0.65 seconds while the average velocity is different.
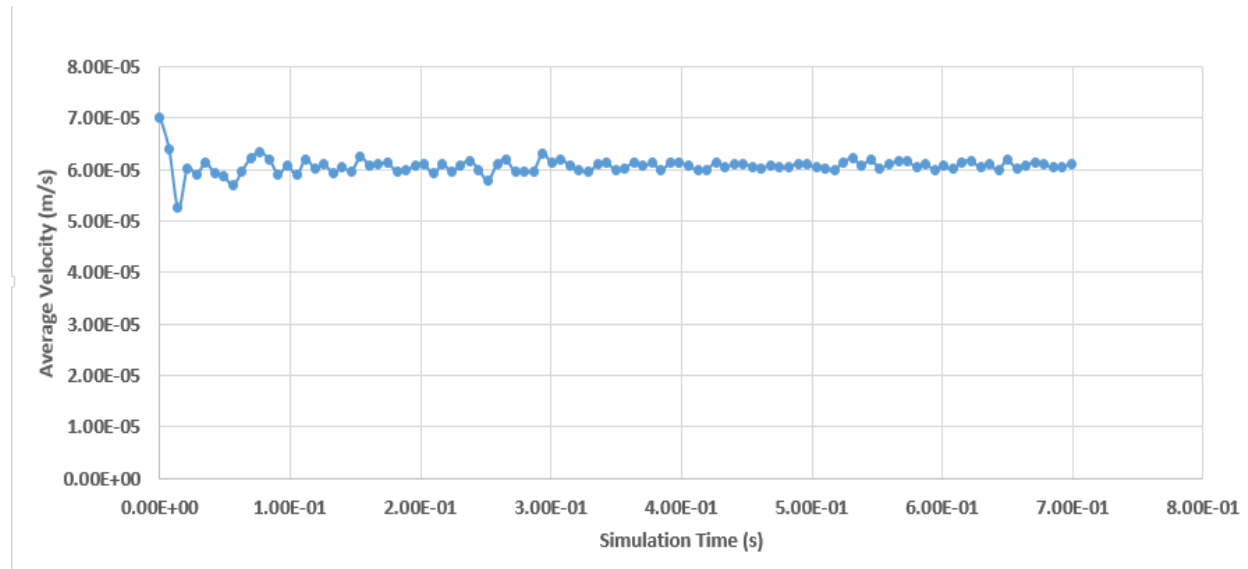
Figure 33-Two particles of 2 micron diameter- Overlapping Particles in range of 10 to 20 nano meters. Average Velocity Vs Simulation Time including Brownian Force
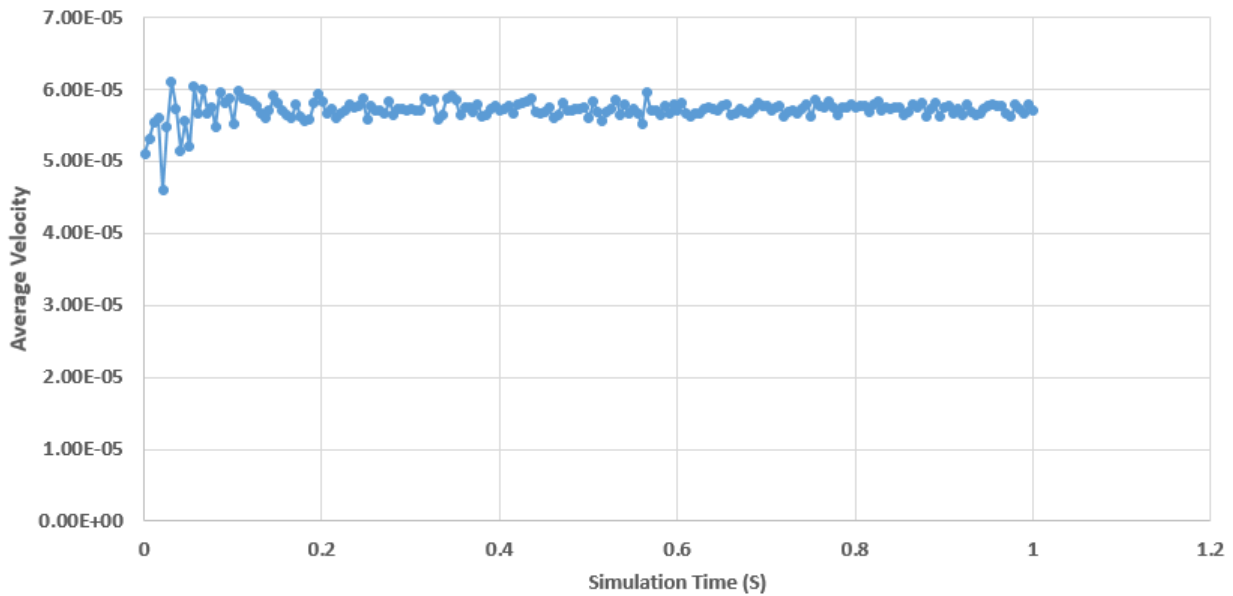
Figure 34- Two particles of 2 micron diameter- Constant distance of 20 nano meters. Average Velocity Vs Simulation Time including Brownian Force

The average velocity of 2 particle chains aggregate is 6.03e-5 m/s when they are overlapping and 5.7e-5 m/s when they keep distance. In both cases these values are almost same as the ones without Brownian motion so as the result if our simulation in micro scale going to be used for the purpose

of visualization of movement and finding the average velocity as the same time for 2 micron scale the simulation run time should be more than 0.7 second. This also means in order to find average velocity for 2 micron particles we can just refer to our simulation without Brownian motion involved.

The situation is completely different in nano scale as we find out that the convergence simulation time is at almost 10 seconds, meaning the average velocity of the chain particles should be gathered from the data of 10 seconds run time simulations at least. This can be a lot time consuming while at the same time shows the effect of Brownian force is dominant in nano scale so our simulation could be running for lower simulations time for visualization purposes of the nano particles movement but to be able to gather data of average velocity in Nano scale it should at least be running for 10 second which as the time-step of our simulation is 10e-9 would be a lot time consuming. Figure 35 shows the average velocity versus simulation time for 1 particle of 500 nano meters.
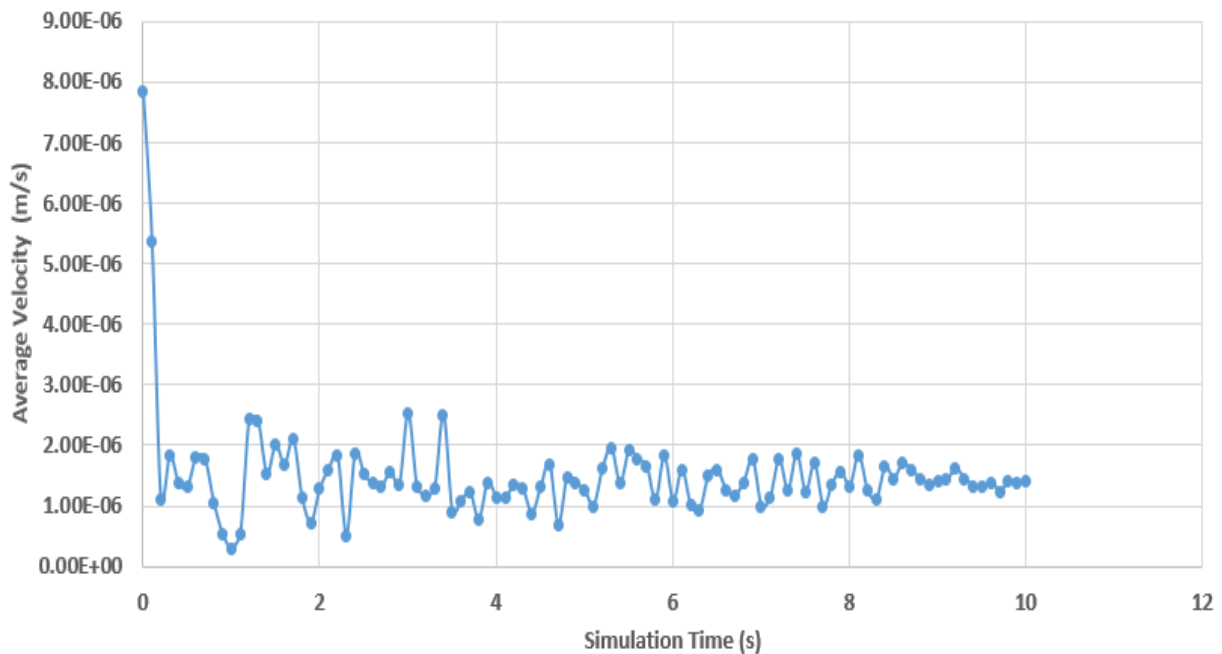
Figure 35 - one particle of 500 nano meters diameter- Average Velocity Vs Simulation Time including Brownian Force

So from the concept mentioned above we did a simulation to find the difference between the average velocity of particles of 2.8 micron with and without the Brownian motion. So for the Simulation to be around converging point of Brownian noise we picked the simulation run time to be 1 second.

The following figures show the average velocity versus magnetic field of 2, 3 and 4 particle aggregates with and without Brownian motion.
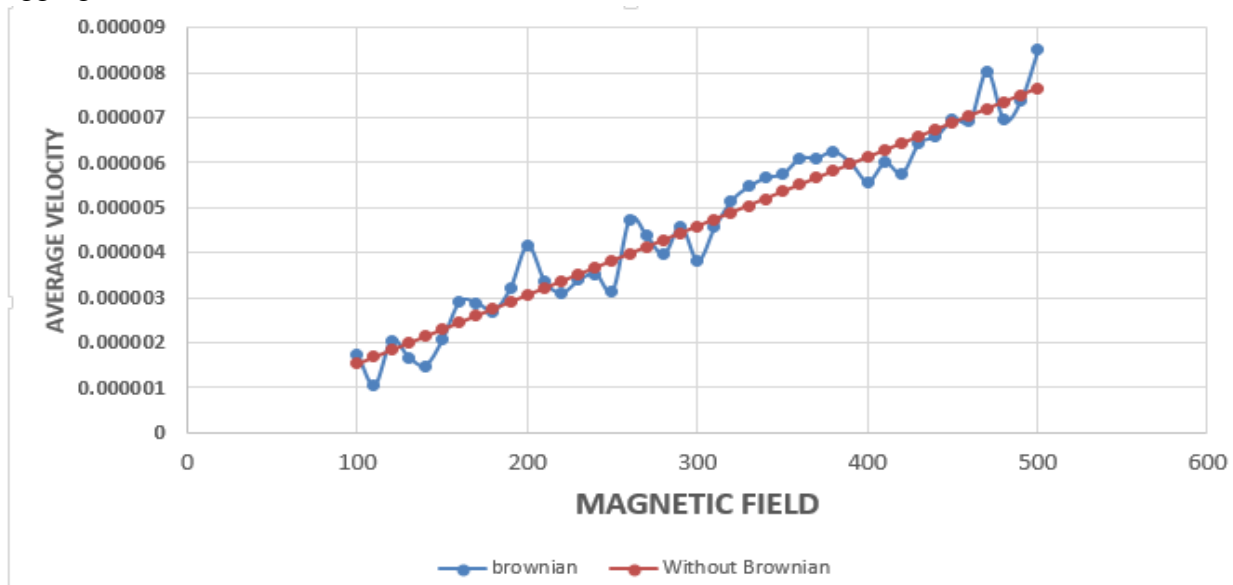
Figure 36 - Average Velocity Vs Magnetic fields- 2.8 micron 2 particles- with and without Brownian motion
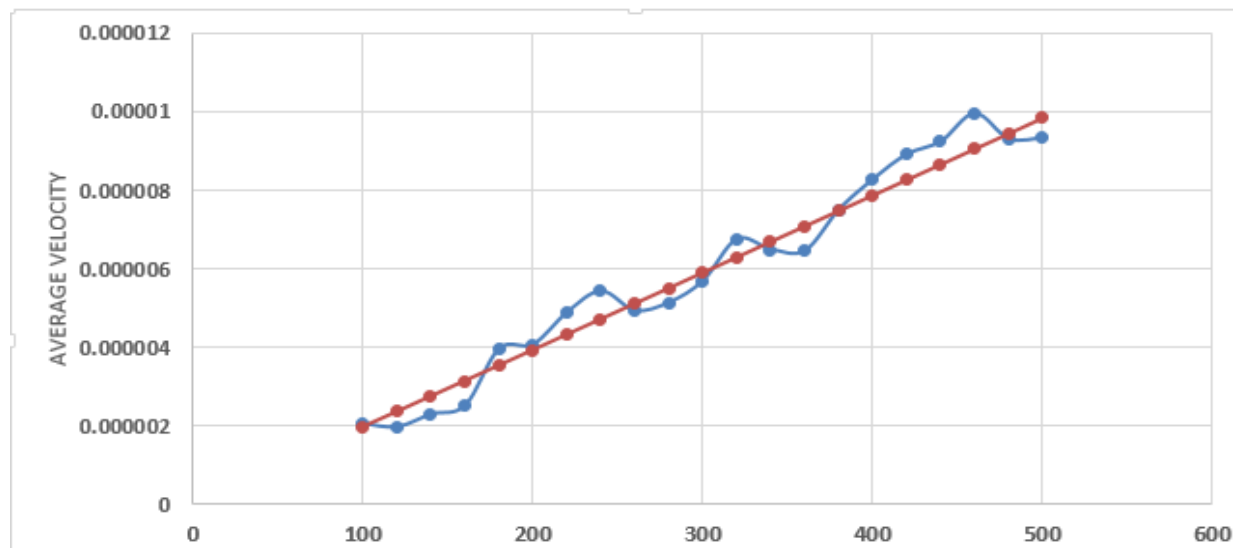
Figure 37 -Average Velocity Vs Magnetic fields- 2.8 micron 3 particles- with and without Brownian motion
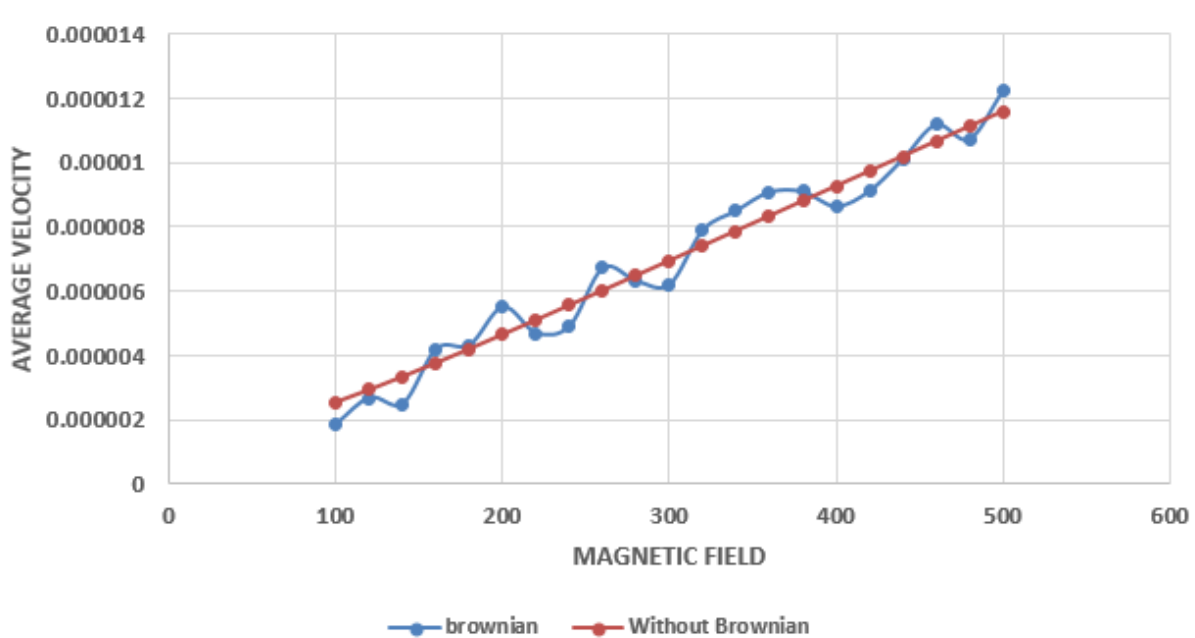
Figure 35 - Average Velocity Vs Magnetic fields- 2.8 micron 4 particles- with and without Brownian motion

So from the figures 36, 37 and 38 it can be seen that the results with Brownian motion are almost as the ones without Brownian motion. The Brownian simulation is not linear which could be expected as the Brownian motion works as a noise. One reason that the results are not completely matching could be that the 1 second simulation time is not exactly the converging point of 2.8 micron particles or the Steric coefficient making the steric force not matching with the Brownian force and as a result making the particles separation not as desired as without Brownian motion.

VI.   Experimental Results

So in this section, using the setup shown in figure 17, we have performed experiments on three different size of Iron oxide Magnetic particles which we had ready and available in our Laboratory. Diluting these magnetic particles powders in water and assigning the fluid viscosity to be *0.0025 Pa.S* and the magnetic permeability of the surrounding medium to be *4πe-7*, we have conducted the experiments in a way to aggregate these chains using a fixed magnetic field parallel to X-Axis of the channel (which was made by gluing two slide glasses on top of each other) and target them along the X axis using the gradient force of the solenoids. Some experimental pictures which have been taken by the Microscope during the experiments for each one of the sizes has been shown in following figures.

Figure 36 – 1 micron particles aggregates after 15 seconds under microscope, Left picture is initial and Right one is Final

Figure 40-2.8 micron particles aggregates after 16 seconds under microscope, Left picture is initial and Right one is Final
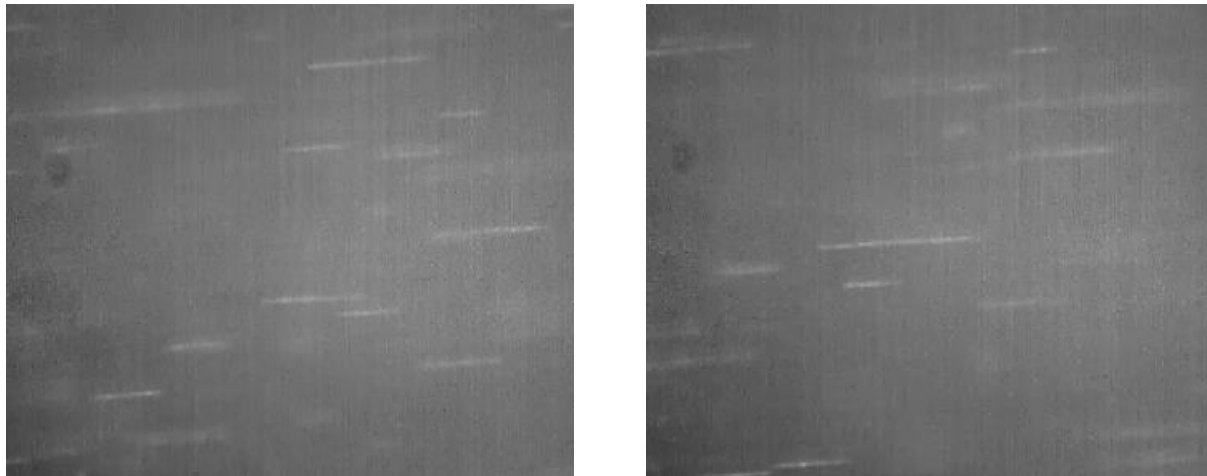
Figure 41-150 nano meter particle aggregates after 16 seconds under microscope, Left picture is initial and Right one is Final
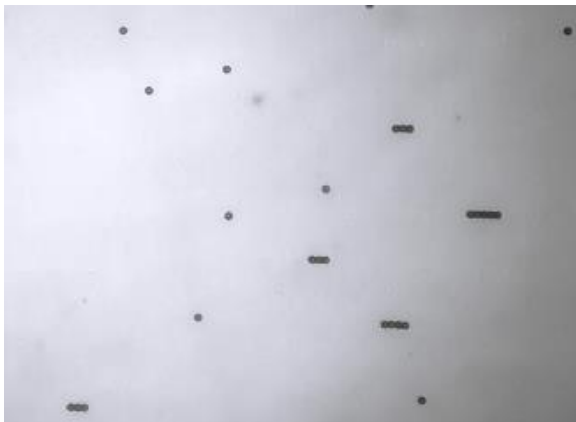
As it can be seen from Figure 41 the white lines show the Nano particles aggregates. We use the dark field technique to image the Particles in Nano scale but still the quality of imaging at Nano scale is quite poor and we can`t exactly find out how many particles in how many rows are gathering together and making the chain. So we approximately assumed them to be linear chains and just counted the number of particles by dividing the chain length to 150 nm which is the particles diameters.

So the experimental result has been shown in the following figures.

Table 4- Experimental Results for 2.8 micron and 1 micron particles at 305 Gauss and 1.6 T/m

Number of particles	2.8 um		Number of particles	1 um	
1	0.618261	AVG	1	AVG	0.369292
	0.100862	STDEV		STDEV	0.081835
2	0.951183	AVG	2	AVG	0.470851
	0.256176	STDEV		STDEV	0.080406
3	0.979422	AVG	3	AVG	0.573325
	0.132364	STDEV		STDEV	0.065772
4	1.142143	AVG	4	AVG	0.600115
	0.142633	STDEV		STDEV	0.101167

Table 5- Experimental Results for 2.8 micron and 1 micron particles at 1160 Gauss and 6.6 T/m

Number of particles	2.8 um		Number of particles	1 um	
1	4.039263	AVG	1	2.759712	AVG
	0.662167	STDEV		0.364399	STDEV
2	5.365728	AVG	2	3.886558	AVG
	0.364441	STDEV		0.551106	STDEV
3	5.910775	AVG	3	4.036092	AVG
	0.717571	STDEV		0.533334	STDEV
4	6.275051	AVG	4	3.726915	AVG
	0.658549	STDEV		0.305352	STDEV

	4um-9um	9um-14um	14um-19.25um
Number of particles in chain	44	76	221
Average Velocity (um/s)	0.209693605	0.335760138	0.406486981
Standard Deviation	0.096658581	0.072072562	0.059068169
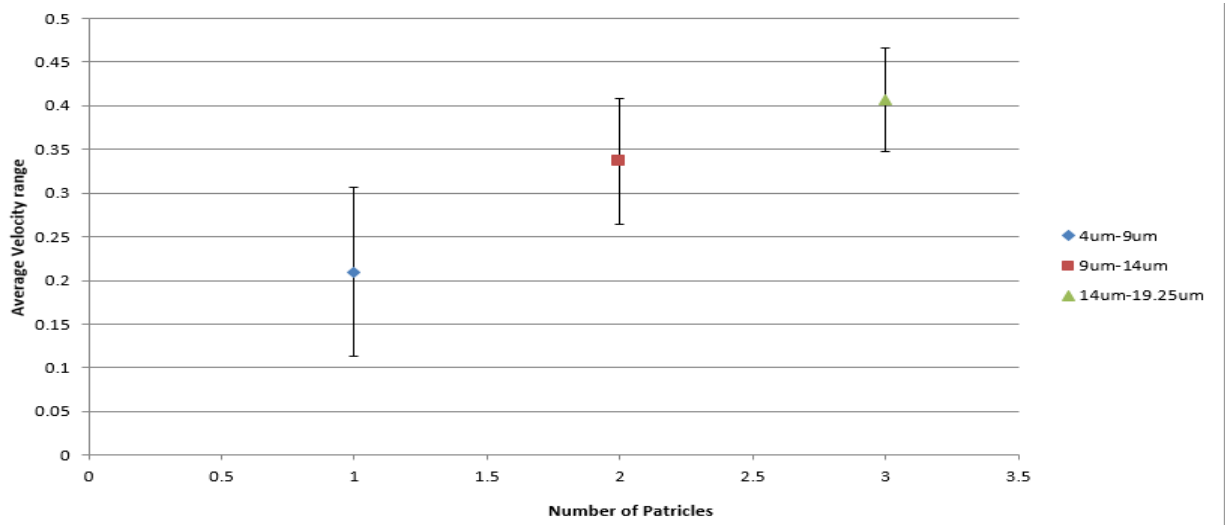
Figure 42- - Experimental Results for Nano particles at 1160 Gauss and 6.6 T/m

Table 7- Simulation Results with correction factors to match the experiments – 305 Gauss, 1.6 T/m

Field	Gradient	1 micron		2.8 micron	
305 Gauss	1.6 T/m	Average Velocity(m/s)	Correction Factors:	Average Velocity(m/s)	Correction Factors:
	N=1	6.04E-07	0.6114	2.77E-06	0.2231
	N=2	1.04E-06	0.4527	4.66E-06	0.20411
	N=3	1.36E-06	0.42156	6.02E-06	0.16269
	N=4	1.60E-06	0.37507	7.06E-06	0.16177

Table 8-Simulation Results with correction factors to match the experiments – 1160 Gauss, 6.6 T/m

Field	Gradient	1 micron		2.8 micron	
1160 Gauss	6.6 T/m	Average Velocity(m/s)	Correction Factors:	Average Velocity(m/s)	Correction Factors:
	N=1	9.48E-06	0.2911	4.35E-05	0.092
	N=2	1.48E-05	0.2626	7.33E-05	0.0732
	N=3	2.15E-05	0.187725	9.46E-05	0.0624
	N=4	2.52E-05	0.147893	1.11E-04	0.05653

⊙   Simulation Results of the same Experiments:

Table 7- Simulation Results with correction factors to match the experiments in Nano scale – 305 Gauss, 1.6 T/m

	4um-9um	9um-14um	14um-19.25um
Number of particles in chain	44	76	111
Average Velocity (um/s)	2.33E+00	2.77E+00	3.05E+00
Correction Factors	0.0899	0.1212	0.13327442

VII.   Visualization in OVITO Software

The goal of our project is to be able to visualize our simulation results similar to imaging videos and figures we capture out of our real imaging system which could be MRI or Microscope. Validating simulation Data by experiments is a part that leads us to be able to present the visualization videos as real time Magnetic Nano/Micro Particles Manipulation systems.

Ovito is the software that captures the Position variables and parameters from Matlab Code simulation and visualize the movement of the aggregate chains in 3D space.

So Ovito can visualize the movement in different aspects and perspectives and develop videos.

The user interface the Ovito software has been shown in the following figure, This could be potentially a design guideline for the user interface of the simulation platform package of DAPS group that will be able to do simulation, Visualization and post processing analysis of Magnetic Particles dynamics of aggregation and breakup. Ideally to get all the input parameters including particle sizes desired magnetic field, Initial and final positions and develop the guideline trajectory by controlling the Magnetic gradient to guide the particles from initial to final position.
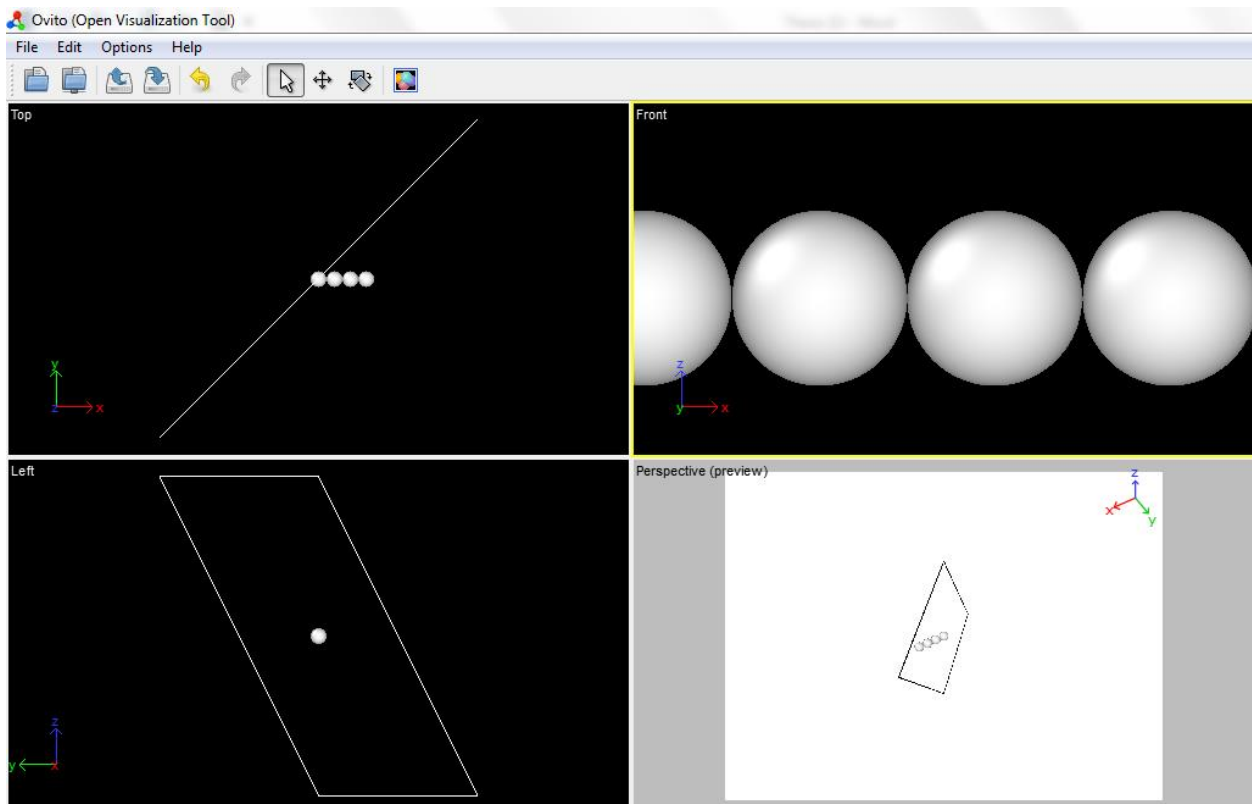
Figure 43 - User interface of the OVITO Visualization software

As the matter of this documents I have provided snapchats of the movies created by Ovito for nano scale particles moving with Brownian motion included in their behavior.
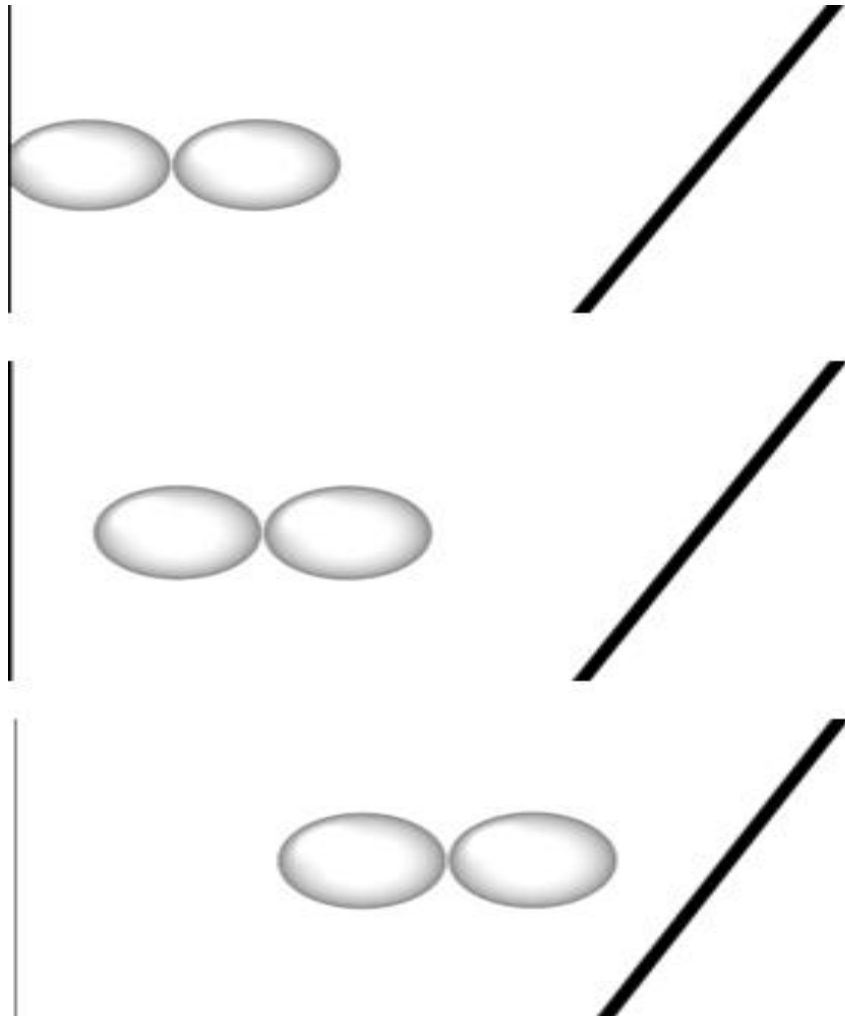
Figure 44 - Visualization in OVITO- 150 nm particles moving with Brownian motion included, The black Diagonal line is the side of an imaginary 2D plane we have drawn in 3D space to show the particles movement more clearly while the Brownian motion which can be seen clearly in the video is hardly to show by this figure but the concept of it has shown clearly on figure 8.

VIII.   Future Work:

In this section the Concepts that the simulations are going to be equipped or expanded on are going to be discussed. Future work will be concentrated on two sides.

First Generating the Control Algorithm that will enable us to control and guide the aggregates within the most efficient trajectory inside the human body.

Secondly applying parallel computation cluster access.

A. Control Algorithm:

To build a control algorithm there are multiple tasks that has to be done:

Task 1: State-space representation: A multi-input and multi-output (MIMO) model will be developed considering the relevant physiological and physical forces. The state-space model will be established from differential equation involving the different magnetic force, drag force, interaction forces, short-range forces… defining the aggregate bolus's dynamic behavior.

Task 2: Identification of the model parameters: The physiological/physical parameters involved in the formation and breakup of the aggregates should be investigated through intensive simulation to identify the control parameters (magnetic field and gradients, shear stress, Newtonian or non-Newtonian blood flow, viscosity, nanoparticle size….). The level of parameter uncertainties and the variability of bolus aggregates (shape and size) will be of prime importance in aggregate control.

Task 3: Synthesis of a robust controller/observer: The forces balance developed in Tasks 1 and 2 will point out that, the model has many parameters highly variable from one person to another. Different robust and adaptive controllers will be tested. The adaptive nonlinear control based on a backstepping approach will perform an *on-line* estimation of some key parameters, while the robust H-infinity controllers will accept bounded uncertainties in model identification, position measurement uncertainties and sensor noise. These controllers will be tested in order to tradeoff the robustness/performance/adaptive characteristics of MRI steering. Furthermore, as blood flow velocity is not measurable, it should be estimated it is actually a challenging issue: if biological parameters are very variable among patients, the pumping blood is also very difficult to estimate (amplitude, mean value and frequency). Various observers such as high-gain observer or Kazantzis-Kravaris Luenberger observer will be tested.

Task 4: Optimization and validation in a Matlab Toolbox: Validation of the proposed controller/observer approach in the Matlab environment for rapid and real-time prototyping.

❖ **Sample Algorithm for Control of the agglomeration`s Displacement:**

The particles are steered by creating a fluid flow that carries all the particles from where they are to where they should be at each time step. Our control loop should comprise sensing, computation, and actuation to steer particles along user-input trajectories. Particle locations are identified in real-time by our simulation results and transferred to a control algorithm that then determines the electrode voltages necessary to create a magnetic flow field or magnetic gradients to carry all the particles to their next desired locations. The process repeats at the next time instant. The controlled magnetic field which actuates the magnetic particle is generated by an arrangement of electromagnets. The set of voltages of these electromagnets represents a control vector. The control design problem is to determine this control vector in terms of the position of the magnetic particle such that the resulting magnetic force drives the particle along any desired trajectory. The magnetic force is a highly nonlinear function of both position and control vector; it sharply drops with distance from the electromagnets and depends quadratically on the control vector. An example of a control system has been shown in figure 45. [9, 10, 34]
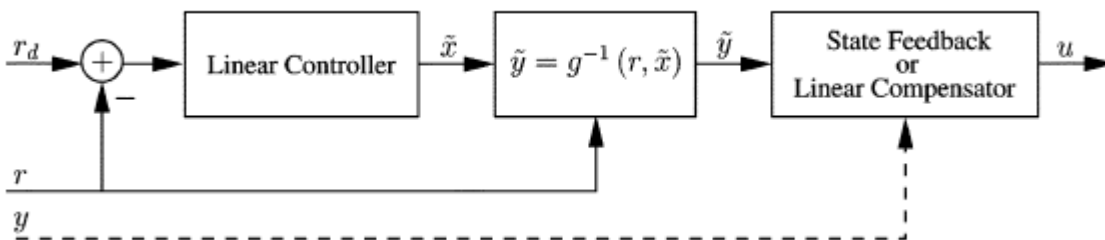

*Figure 45 -Structure of a nonlinear controller with compensation for the bandwidth of the subsystem. Our control loop should comprise sensing, computation, and actuation to steer particles along user-input trajectories (**Reference 9**)*

B. - Parallel Computing:

Simulations are time consuming, power consuming and heat generating even for a high speed PC so faster computation is needed. The most logical solution is parallel computing, a form of computation in which many calculations are carried out simultaneously, operating on the principle that large problems can often be divided into smaller ones, which are then solved concurrently. This has become the dominant paradigm in computer architecture, mainly in the form of multicore processors.

To perform parallel computing. A different processor will compute each thread. Either the multi-core capabilities of CPUs or GPUs or a cluster of CPUs may be used to concurrently perform the multithread tasks. The most popular and cost-effective approach to parallel computing is cluster computing.

*Figure 46 -Schematic of Generic Parallel Computer (GPC). It shows how any running program or simulation can be divided into multiple sections to run on different memory parts and the results will be gathered by the main program resulting in higher runtime speed. (**Referenced from Google Image**)*

Fortunately Northeastern University has a new operating system called discovery cluster which enables us students to run multiple simulations on it at the same time. While it is running simulations on a super computer the runtime of each simulation decreases rapidly which is very important for our simulations especially in NANO scale. [11, 12]
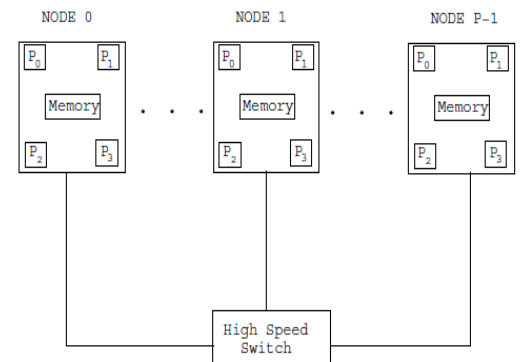
IX. References

[1] Pierre Pouponneau, Jean-Christophe Leroux, Sylvain Martel, "Magnetic nanoparticles encapsulated into biodegradable microparticles steered with an upgraded magnetic resonance imaging system for tumor chemoembolization", Biomaterials, Vol. 30 (31) 2009, pp. 6327-6332.

[2] Vartholomeos P., M. Fruchard, A. Ferreira, and C. Mavroidis, "MRI Guided Nanorobotic Systems for Therapeutic and Diagnostic Applications", Annual Review of Biomedical Engineering, Vol. 13: 157-184, (August 2011).

[3] Vartholomeos P. D. Mavroidis, "Simulation Platform for Self-assembly Structures in MRI-guided Nanorobotic Drug Delivery Systems", IEEE International Conference on Robotics and Automation, Alaska, May 2010, pp. 5594-5600.

[4] Sylvain Martel, Ouajdi Felfoul, Jean-Baptiste Mathieu, Arnaud Chanu, Samer Tamaz, Mahmood Mohammadi, Martin Mankiewicz, and Nasr Tabatabaei, "MRI-based Medical Nanorobotic Platform for the Control of Magnetic Nanoparticles and Flagellated Bacteria for Target Interventions in Human Capillaries", Int. J. Rob. Res. 2009 September 1; 28(9): 1169–1182.

[5] Panagiotis Vartholomeos, Matthieu Fruchard, Antoine Ferreira and Constantinos Mavroidis "MRI-Guided Nanorobotic Systems for Therapeutic and Diagnostic Applications "

[6] Panagiotis Vartholomeos and Constantinos Mavroidis "In-silico studies of micro magnetic particle aggregation in fluid environments for MRI guided drug delivery"

[7] Robert W. Barber, David R. Emerson *"Optimal design of microfluidic networks using biologically inspired principles".*

[8] Michael P. Kummer, Student Member, IEEE, Jake J. Abbott, Member, IEEE, Bradley E. Kratochvil, Member, IEEE, Ruedi Borer, Ali Sengul, Student Member, IEEE, and Bradley J. Nelson, Senior Member, IEEE. "*OctoMag*: An Electromagnetic System for 5-DOF Wireless Micromanipulation".

[9] Arash Komaee, Member, IEEE, and Benjamin Shapiro. "Steering a Ferromagnetic Particle by Optimal Magnetic Feedback Control".

[10] Satej Chaudhary and Benjamin Shapiro. "Arbitrary Steering of Multiple Particles Independently in an Electro-Osmotically Driven Microfluidic System".

[11] George Em Karniadakis and Robert M. Kirby "Parallel Scientific Computing in C++ and MPI".

[12] Yusuke Shigeto, Mikio Sakai, Parallel computing of discrete element method on multi-core processors, Particuology, Volume 9, Issue 4, August 2011.

[13] Thorsten Poschel, Thomas Schwager, Computational Granular Dynamics: Models and Algorithms, Springer, Berlin, 2005, pp 17-67.

[14] Netanel Korin, Mathumai Kanapathipillai, Benjamin D. Matthews, Marilena Crescente, Alexander Brill, Tadanori Mammoto, Kaustabh Ghosh, Samuel Jurek, Sidi A. Bencherif, Deen Bhatta, Ahmet U. Coskun, Charles L. Feldman, Denisa D. Wagner,4,5 Donald E. "Shear-Activated Nano therapeutics for Drug Targeting to Obstructed Blood Vessels"

[15] Y. Gao, M.A. Hulsen and J.M.J. den Toonder "DYNAMICS OF ROTATING MAGNETIC MICRO-BEAD CHAINS"

[16] Ioannis Petousis, Erik Homburg, Roy Derks and Andreas Dietzel "Transient behavior of magnetic micro-bead chains rotating in a fluid by external fields"

[17] Anil K. Vuppu, Antonio A. Garcia, and Mark A. Hayes "Video Microscopy of Dynamically Aggregated Paramagnetic Particle Chains in an Applied Rotating Magnetic Field"

[18] Kenji Iimura, SatoshiWatanabe, MichitakaSuzuki, MitsuakiHirota, KoHigashitani "Simulation of entrainment of agglomerates from plate surfaces by shear flows"

[19] Jin-Wook Yoo, Darrell J. Irvine, Dennis E. Discher, & Samir Mitragotri, "Bio-inspired, bioengineered and biomimetic drug delivery carriers", Nature Reviews Drug Discovery 10, 521-535 (July 2011).

[20] S. C. Glotzer, M. J. Solomon, and N. A. Kotov, "Self-Assembly: From Nanoscale to Microscale Colloids", AIChE Journal, Vol. 50, No. 12, 2004.

[21] Takami Yamaguchi, Takuji Ishikawa, Y. Imai, N. Matsuki, Mikhail Xenos, Yuefan Deng, and Danny Bluestein, "Particle-Based Methods for Multiscale Modeling of Blood Flow in the Circulation and in Devices: Challenges and Future Directions", Ann Biomed Eng. 2010 March; 38(3): 1225–1235.

[22] B. H. Han, S. Park and S. Y. Lee, "Gradient waveform synthesis for magnetic propulsion using MRI gradient coils", Physics in Medicine and Biology, Volume 53, Number 17, 2008, pp. 4639.

[23] J. M. Haile, Molecular Dynamics Simulation, John Wiley & Sons, Inc, 1997.

[24] R. Engel-Herberta, and T. Hesjedal, "Calculation of the magnetic stray field of a uniaxial magnetic domain", J. of Applied Physics 97, 074504, 2005.

[25] C.N Likos, H. Lowen, M. Watzlawek, B.Abbas, O. Juckinschke, J. Allgaier, And D. Richter Phys. Star Polymers Viewed as Ultrasoft Colloidal Particles.

[26] Jean-Baptiste Mathieu and Sylvain Martel, "Steering of Aggregating Magnetic Microparticles Using Propulsion Gradients Coils in an MRI Scanner", Magnetic Resonance in Medicine 63:1336–1345 (2010).

[27] Jae-Hyun Lee, Jung-tak Jang, Jin-silChoi, Seung Ho Moon, Seung-hyun Noh, Ji-wook Kim, Jin-Gyu Kim, Il-Sun Kim, Kook In Park and Jinwoo Cheon . Exchange-coupled magnetic nanoparticles for efficient heat induction"

[28] Eldin Wee Chuan Lim and Ruili Feng "Agglomeration of magnetic nanoparticles".

[29] Zhengbiao Peng, Elham Doroodchi, Geoffrey Evans. "DEM simulation of aggregation of suspended nanoparticles".

[30] A. Weddemann, F. Wittbracht, A. Auge, A. Hutten."Particle flow control by induced dipolar interaction of superparamagnetic microbeads".

[31] Manuel Arruebo, Rodrigo Fernández-Pacheco, Panagiotis Vartholomeos, Matthieu Fruchard, Antoine Ferreira and Constantinos Mavroidis. "Magnetic nanoparticles for drug delivery"

[32] Andrew L. Richards, Clement Kleinstreuer, Andrew S. Kennedy, Emily Childress, and Gregory D. Buckner "*Experimental Microsphere Targeting in a Representative Hepatic Artery System*". Ricardo Ibarra, and Jesús Santamaría*

[33] Challa S.S.R. Kumar, Faruq Mohammad. "Magnetic nano materials for hyperthermia-based therapy and controlled drug delivery"

[34] Arcese L., M. Fruchard and A. Ferreira, "Nonlinear modeling and robust controller-observer for magnetic microrobot in a fluidic environment using MRI gradients," Proc. IEEE International Conf. on Intelligent Robotics and Systems, St. Louis, USA, 2009.

[35] Kar W. Yung, Peter B. Landecker and Daniel D. Villani, "An analytic solution for forces between two magnetic dipoles", Magnetic and Electrical Separation, Vol. 9, pp. 39-52, 1998.

[36] J. D. Jackson, "Classical Electrodynamics", 3rd ed., John Wiley & Sons, Inc, pp. 184-190, 1999.

[37] F. M White, Fluid Mechanics, 5th Ed., McGraw-Hill Science, 2002.

[38] Engineering Nano medicines for Improved Melanoma Therapy: Progress and Promises. Di Bei; Jianing Meng; Bi-Botti C Youan.